Article

The Hydrogen Chemistry of the FeMo-co Active Site of Nitrogenase

Ian Dance

J. Am. Chem. Soc., **2005**, 127 (31), 10925-10942• DOI: 10.1021/ja0504946 • Publication Date (Web): 19 July 2005

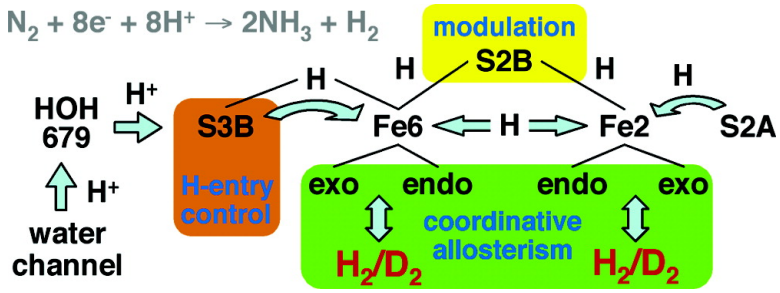

More About This Article

Additional resources and features associated with this article are available within the HTML version:

- Supporting Information
- Links to the 8 articles that cite this article, as of the time of this article download
- Access to high resolution figures
- Links to articles and content related to this article
- Copyright permission to reproduce figures and/or text from this article

View the Full Text HTML

J|A|C|S
ARTICLES
Published on Web 07/19/2005

The Hydrogen Chemistry of the FeMo-co Active Site of Nitrogenase

Ian Dance*

Contribution from the School of Chemistry, University of New South Wales, Sydney 2052, Australia

Received January 25, 2005; E-mail: i.dance@unsw.edu.au

Abstract: The chemical mechanism by which nitrogenase enzymes catalyze the hydrogenation of N_2 (and other multiply bonded substrates) at the $N^cFe_7MoS_9$(homocitrate) active site (FeMo-co) is unknown, despite the accumulation of much data on enzyme reactivity and the influences of key amino acids surrounding FeMo-co. The mutual influences of H_2, substrates, and the inhibitor CO on reactivity are key experimental tests for postulated mechanisms. Fundamental to all aspects of mechanism is the accumulation of H atoms (from $e^- + H^+$) on FeMo-co, and the generation and influences of coordinated H_2. Here, I argue that the first introduction of H is via a water chain terminating at water 679 (PDB structure 1M1N, *Azotobacter vinelandii*) to one of the μ_3-S atoms (S3B) of FeMo-co. Next, using validated density functional calculations of a full chemical representation of FeMo-co and its connected residues (α-275^{Cys}, α-442^{His}), I have characterized more than 80 possibilities for the coordination of up to three H atoms, and H_2, and $H + H_2$, on the S2A, Fe2, S2B, Fe6, S3B domain of FeMo-co, which is favored by recent targeted mutagenesis results. Included are calculated reaction profiles for movements of H atoms (between S and Fe, and between Fe and Fe), for the generation of $Fe-H_2$, for association and dissociation of $Fe-H_2$ at various reduction levels, and for H/H_2 exchange. This is new hydrogen chemistry on an unprecedented coordination frame, with some similarities to established hydrogen coordination chemistry, and with unexpected and unprecedented structures such as $Fe(S)_3(H_2)_2(H)$ octahedral coordination. General principles for the hydrogen chemistry of FeMo-co include (1) the stereochemical mobility of H bound to μ_3-S, (2) the differentiated endo- and exo- positions at Fe for coordination of H and/or H_2, and (3) coordinative allosteric influences in which structural and dynamic aspects of coordination at one Fe atom are affected by coordination at another Fe atom, and by H on S atoms. Evidence of end-differentiation in FeMo-co is described, providing a rationale for the occurrence of Mo. The reactivity results are discussed in the context of the Thorneley−Lowe scheme for nitrogenase reactions, and especially the scheme for the HD reaction ($2H^+ + 2e^- + D_2 \rightleftharpoons 2HD$), using a model containing an H-entry site and at least two coordinative sites on FeMo-co. I propose that S3B is the H-entry site, suggest details for the H^+ shuttle to S3B and subsequent movement of H atoms around FeMo-co preparatory to the binding and hydrogenation of N_2 and other substrates, and suggest how H could be transferred to an alkyne substrate. I propose that S2B (normally hydrogen bonded to α-195^{His}) has a modulatory function and is not an H-entry site. Finally, the recent first experimental trapping of a hydrogenated intermediate with EPR and ENDOR characterization is discussed, leading to a consensual model for the intermediate.

Introduction

The enzyme nitrogenase catalyses the reduction of dinitrogen to ammonia under conditions much milder than any laboratory or industrial process, but the chemical mechanism by which this is achieved is still enigmatic. Current knowledge of the enzyme includes (1) the structures of the proteins involved,[1−3] (2) the structure of the iron−molybdenum cofactor (FeMo-co) which is the site of catalysis,[4] (3) the biochemical sequences of protein docking events that introduce the electrons used in the reduction,[5−10] (4) the behavior with alternative substrates, and inhibitors,[8,11] and (5) the effects of mutation of key residues surrounding FeMo-co.[7,9,10,12,13] The FeMo-co active site (Figure 1) is a NFe_7MoS_9(homocitrate) cluster linked to the protein through a cysteine residue coordinated to iron and a histidine residue coordinated to molybdenum (Figure 1).[14] The central trigonal prism of six iron atoms (Fe2−Fe7) linked by three doubly bridging sulfur atoms and centered by a small atom,

(1) Kim, J.; Rees, D. C. *Science* **1992**, *257*, 1677−1682. Kim, J.; Rees, D. C. *Nature* **1992**, *360*, 553−560. Georgiadis, M. M.; Komiya, H.; Chakrabarti, P.; Woo, D.; Kornuc, J. J.; Rees, D. C. *Science* **1992**, *257*, 1653−1659. Chan, M. K.; Kim, J.; Rees, D. C. *Science* **1993**, *260*, 792−794. Bolin, J. T.; Ronco, A. E.; Morgan, T. V.; Mortenson, L. E.; Xuong, N. H. *Proc. Natl. Acad. Sci. U.S.A.* **1993**, *90*, 1078−1082. Bolin, J. T.; Campobasso, N.; Muchmore, S. W.; Mortenson, L. E.; Morgan, T. V. *J. Inorg. Biochem.* **1993**, *51*, 356. Rees, D. C.; Chan, M. K.; Kim, J. *Adv. Inorg. Chem.* **1993**, *40*, 89−119. Kim, J.; Rees, D. C. *Biochemistry* **1994**, *33*, 389−397. Grossman, J. G.; Hasnain, S. S.; Yousafzai, F. K.; Smith, B. E.; Eady, R. R. *J. Mol. Biol.* **1997**, *266*, 642−648. Schlessman, J. L.; Woo, D.; Joshua-Tor, L.; Howard, J. B.; Rees, D. C. *J. Mol. Biol.* **1998**, *280*, 669−685. Smith, B. E. *Adv. Inorg. Chem.* **1999**, *47*, 159−218.
(2) Howard, J. B.; Rees, D. C. *Chem. Rev.* **1996**, *96*, 2965−2982.
(3) Mayer, S. M.; Lawson, D. M.; Gormal, C. A.; Roe, S. M.; Smith, B. E. *J. Mol. Biol.* **1999**, *292*, 871−891.

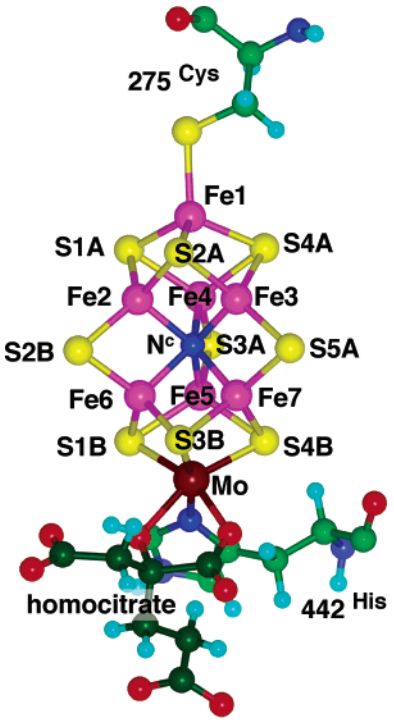

Figure 1. The structure of FeMo-co, connected to the protein via α-275^{Cys} and α-442^{His} (*Azotobacter vinelandii*), with atom labeling for crystal structure 1M1N. In this and following figures, the C atoms of homocitrate are dark green.

probably nitrogen (N^c), is a chemically unusual structure, which attracts attention as the domain for the reactions of nitrogenase. Recent biochemical investigations with specifically modified proteins and substrates have provided strong evidence that the Fe_4 face of FeMo-co involving atoms Fe2,Fe3,Fe6,Fe7 is where alkynes and alkenes are bound,[15−17] and these biochemical data have been elaborated with computational modeling.[18] There are inhibitory relationships between alkyne and dinitrogen substrates, and so this face is implicated also in the dinitrogen chemistry.[17]

Scheme 1. A Modified Presentation of the Thorneley−Lowe Scheme To Account for the Kinetics of Nitrogenase[a]

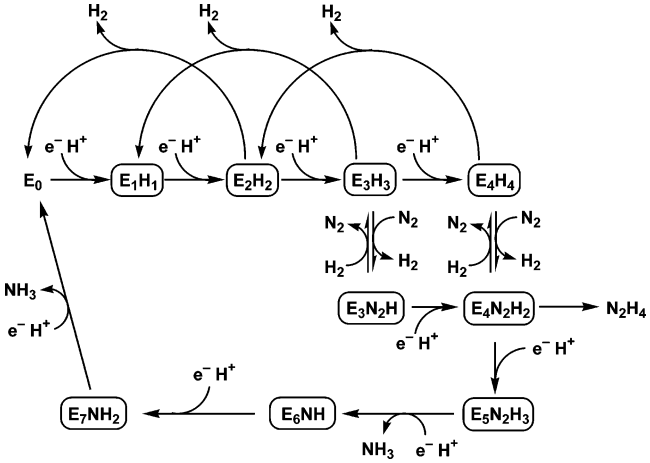

[a] The formulas of the intermediates, enclosed, signify only composition, not structure.

Nitrogenase uses electrons and protons to hydrogenate N_2, and all other substrates. This requires careful chemical control, to direct electrons and protons toward recalcitrant substrates while avoiding the facile combination of electrons and protons to form H_2. There is always some leakage to H_2 (obligatory hydrogen evolution), depending on the substrate and the ratio of electron flux to substrate availability. In practice, experimental monitoring of H_2 evolution is a useful indicator of the efficacy and activity of combinations of substrates with wild type or modified enzymes.

There are extensive experimental data about the hydrogen reactivity of nitrogenase. Much of this is embodied in Scheme 1, developed by Thorneley and Lowe from their detailed kinetic data, and explaining many other observations.[5] This scheme involves eight stages of linked electronation and protonation during the cycle, labeled E_0 to E_7. The earlier stages of reduction are the more intriguing, involving the accumulation of H atoms on FeMo-co, the evolution of H_2, and the initial binding of N_2, and these compositions of the intermediates are indicated on the scheme. The first participation of N_2 occurs at E_3 and E_4, in equilibria involving interchange with H_2 reflecting the fact that H_2 is a competitive inhibitor of the reduction of N_2.

Scheme 1 implies at least nine intermediates. Trapping and direct measurement of early intermediates is difficult, due to reversionary elimination of H_2, but EPR and ENDOR measurements of E_2H_2 have recently been reported[19] for the α-70^{Ile} mutant.[17] Insight into the nature of the intermediates comes from kinetic analysis of the HD formation reaction of nitrogenase, which is the N_2-dependent formation of HD in the presence of D_2.[5,8,20−22] When nitrogenase turns over under D_2, HD is formed, but only in the presence of N_2: alternative substrates such as

(4) Einsle, O.; Tezcan, F. A.; Andrade, S. L. A.; Schmid, B.; Yoshida, M.; Howard, J. B.; Rees, D. C. *Science* **2002**, *297*, 1696−1700.
(5) Thorneley, R. N. F.; Lowe, D. J. In *Molybdenum enzymes*; Spiro, T. G., Ed.; Wiley-Interscience: New York, 1985; pp 221−284.
(6) Howard, J. B.; Rees, D. C. *Annu. Rev. Biochem.* **1994**, *63*, 235−264. Seefeldt, L. C.; Dean, D. R. *Acc. Chem. Res.* **1997**, *30*, 260−266.
(7) Peters, J. W.; Fisher, K.; Dean, D. R. *Annu. Rev. Microbiol.* **1995**, *49*, 335−366.
(8) Burgess, B. K.; Lowe, D. J. *Chem. Rev.* **1996**, *96*, 2983−3011.
(9) Christiansen, J.; Dean, D. R.; Seefeldt, L. C. *Annu. Rev. Plant Physiol. Plant Mol. Biol.* **2001**, *52*, 269−295.
(10) Igarashi, R. Y.; Seefeldt, L. C. *Crit. Rev. Biochem. Mol. Biol.* **2003**, *38*, 351−384.
(11) Burris, R. H. *J. Biol. Chem.* **1991**, *266*, 9339−9342. Yates, M. G. In *Biological Nitrogen Fixation*; Stacey, G., Burris, R. H., Evans, H. J., Eds.; Chapman and Hall: New York, 1992; pp 685−735. Seefeldt, L. C.; Rasche, M. E.; Ensign, S. A. *Biochemistry* **1995**, *34*, 5382−5389. McKenna, C. E.; Simeonov, A. M.; Eran, H.; Bravo-Leerabhandh, M. *Biochemistry* **1996**, *35*, 4502−14. Christie, P. D.; Lee, H. I.; Cameron, L. M.; Hales, B. J.; Orme-Johnson, W. H.; Hoffman, B. M. *J. Am. Chem. Soc.* **1996**, *118*, 8707−8709. Lee, H. I.; Cameron, L. M.; Hales, B. J.; Hoffman, B. M. *J. Am. Chem. Soc.* **1997**, *119*, 10121−10126. Cameron, L. M.; Hales, B. J. *Biochemistry* **1998**, *37*, 9449−9456. Maskos, Z.; Hales, B. J. *J. Inorg. Biochem.* **2003**, *93*, 11−17. McLean, P. A.; True, A.; Nelson, M. J.; Lee, H.-I.; Hoffman, B. M.; Orme-Johnson, W. H. *J. Inorg. Biochem.* **2003**, *93*, 18−32.
(12) Fisher, K.; Dilworth, M. J.; Kim, C.-H.; Newton, W. E. *Biochemistry* **2000**, *39*, 2970−2979.
(13) Fisher, K.; Dilworth, M. J.; Newton, W. E. *Biochemistry* **2000**, *39*, 15570−15577.
(14) Atom and residue numbering used in this paper are those of *Azotobacter vinelandii* and crystal structure 1M1N.
(15) Christiansen, J.; Seefeldt, L. C.; Dean, D. R. *J. Biol. Chem.* **2000**, *275*, 36104−36107.
(16) Mayer, S. M.; Niehaus, W. G.; Dean, D. R. *J. Chem. Soc., Dalton Trans.* **2002**, 802−807. Benton, P. M. C.; Laryukhin, M.; Mayer, S. M.; Hoffman, B. M.; Dean, D. R.; Seefeldt, L. C. *Biochemistry* **2003**, *42*, 9102−9109. Lee, H.-I.; Igarashi, R.; Laryukhin, M.; Doan, P. E.; Dos Santos, P. C.; Dean, D. R.; Seefeldt, L. C.; Hoffman, B. M. *J. Am. Chem. Soc.* **2004**, *126*, 9563−9569. Igarashi, R.; Dos Santos, P. C.; Niehaus, W. G.; Dance, I. G.; Dean, D. R.; Seefeldt, L. C. *J. Biol. Chem.* **2004**, *279*, 34770−34775.
(17) Barney, B. M.; Igarashi, R. Y.; Dos Santos, P. C.; Dean, D. R.; Seefeldt, L. C. *J. Biol. Chem.* **2004**, *279*, 53621−53624.
(18) Dance, I. *J. Am. Chem. Soc.* **2004**, *126*, 11852−11863.
(19) Igarashi, R. Y.; Laryukhin, M.; Dos Santos, P. C.; Lee, H.-I.; Dean, D. R.; Seefeldt, L. C.; Hoffman, B. M. *J. Am. Chem. Soc.* **2005**, *127*, 6231−6241.

Scheme 2. The Thorneley−Lowe Reaction Scheme (Amended) for the HD Formation Reaction, Based on Levels E_1−E_3 of Scheme 1[a]

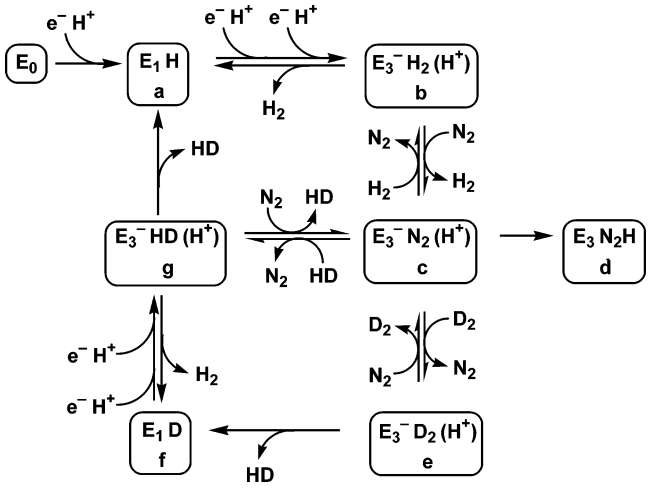

[a] (H^+) signifies the differentiated protonic site (see text). Reduction of N_2 and obligatory H_2 evolution proceed through intermediates **a** → **b** → **c** → **d**; general H_2 evolution is by **a** ↔ **b**; N_2-dependent formation of HD from D_2 involves **c** → **e** → **f** → **g** → **a**,**c**. Direct H_2/D_2 exchange between **b** and **e** is not included because it is kinetically uncompetitive with the pathway involving **c**.

Scheme 3. Generalized Model for the Coordination Positions and the Differentiated H-Entry Site Involved in the Formulation of Structural Hypotheses about the Mechanisms of the N_2-Promoted HD Reaction of Nitrogenase (Scheme 2) and the Reduction of N_2[a]

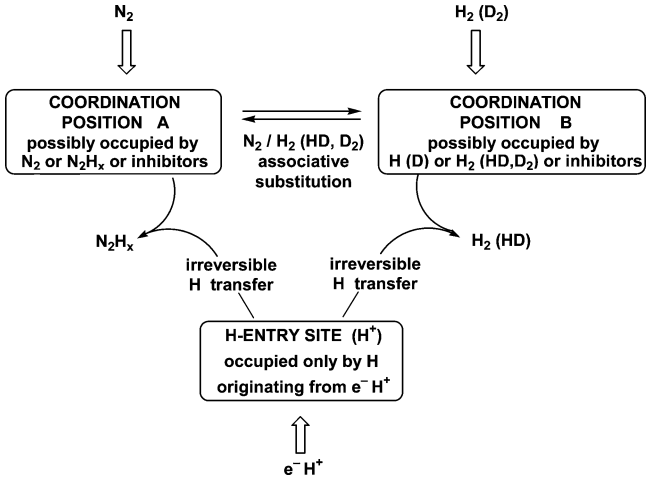

[a] The entry site accepts the proton that comes with electron transfer to FeMo-co. This H atom, which is exchangeable with solvent, can be transferred to an H(D) or N atom at one of the coordination positions (or to a vacant coordination position). Reverse transfer from a coordination position to the H-entry site is forbidden by the kinetics. The coordinative positions bind H_2 (D_2) or N_2, or inhibitors, and release products.

C_2H_2, N_3^-, or N_2O do not enable the formation of HD. The HD formation is not catalyzed H_2/D_2 exchange, but is a reduction, with stoichiometry $2H^+ + 2e^- + D_2 \Rightarrow 2HD$. Further, during turnover under HD, D_2 is not formed. In addition, when T_2 is used, there is negligible leakage of T^+ into the aqueous phase.[20] Reaction Scheme 2 (an elaborated subset of Scheme 1) has been presented by Thorneley and Lowe to explain these properties of the N_2-dependent HD formation reaction at the E_1−E_3 levels.[5,8,23]

A necessary feature of this reaction scheme is the occurrence of a site (marked (H^+) in Scheme 2) that is occupied by the incoming proton at each cycle of electronation and protonation. This proton can transfer to either of the other two bound atoms and be included in released H_2 or HD, or in the reduction products of N_2, but it cannot exchange with D_2 (T_2) or HD. Another key kinetic characteristic of reaction Scheme 2 is that H_2/D_2 exchange between **b** and **e** is only kinetically competitive when it passes through **c**: this accounts for the observation that the steady-state kinetics of HD formation and of the inhibition of N_2 reduction by H_2 are the same.[5,8,23]

In this way, the kinetic data are providing clues about the differentiation of binding locations for hydrogen atoms and molecules, and of N_2 and its reduced intermediates. In proceeding to interpret this reaction scheme in terms of structures for the intermediates, it is necessary to think in terms of a number of coordination positions (for H (D) atoms, H_2 (HD, D_2) molecules, N_2 molecules, and N_2H_x intermediates) as well as the differentiated (H^+) site of Thorneley and Lowe, which I call the "H-entry site". In view of the associative exchange reactions in Schemes 1 and 2, and the influences of exogenous inhibitors such as CO, a minimum of two coordination positions is expected, and Scheme 3 outlines the conceptual framework for structural hypotheses about the intermediates. There are two coordination positions that bind H (D), H_2 (HD, D_2), N_2, or N_2H_x species, and that facilitate the associative exchange of N_2 with H_2 (or isotopomers). H atoms enter the system only via the entry site, from which they transfer irreversibly to atoms at the coordinative positions, forming and releasing H_2 (or HD) or forming N_2H_x intermediates that then proceed (by repetition of the cycle) to the N_2H_4 or NH_3 products. H atoms at the H-entry site are readily exchangeable with solvent, but those at the coordination positions are less so. The different reduction levels (E_1, E_2, E_3, etc.) are described by the total of the H atoms accumulated at all sites and H atoms transferred to substrate. An ancillary concept that becomes important in evaluating the mutual reactivity data for FeMo-co with N_2, C_2H_2, and CO is that a coordination position changes according to the reduction level.[9]

This brief description of some aspects of the hydrogen chemistry of nitrogenase is sufficient to indicate that (1) there must be a number of different binding sites for various numbers of H atoms and of substrate in various stages of hydrogenation, and (2) these sites must be such that some H transfer reactions have low barriers and some have insurmountable barriers. As already indicated, direct experimental observation of these intermediates is difficult and has only recently been achieved.[19] To make progress, basic information about the hydrogen chemistry of FeMo-co is needed. The objective of this paper is to develop the fundamental and distinctive hydrogen coordination chemistry of FeMo-co, using reliable theoretical methods and the full FeMo-co structure. There is now an impressive amount of information and understanding of the hydrogen chemistry of standard coordination and organometallic compounds,[24−26] which, together with density functional (DF) calculations on model systems,[27−32] has been used to generate speculative models for the action of nitrogenase.[22,31−33] How-

(20) Burgess, B. K.; Wherland, S.; Newton, W. E.; Stiefel, E. I. *Biochemistry* **1981**, *20*, 5140−5146.
(21) Li, J.-L.; Burris, R. H. *Biochemistry* **1983**, *22*, 4472−4480.
(22) Sellmann, D.; Fursattel, A.; Sutter, J. *Coord. Chem. Rev.* **2000**, *200*−*202*, 545−561.
(23) Lowe, D. J.; Thorneley, R. N. F. *Biochem. J.* **1984**, *224*, 895−901.

ever, FeMo-co has an unprecedented and distinctive structure and is likely to have a distinctive hydrogen chemistry.[34]

Of the large number of theoretical investigations of aspects of FeMo-co, density functional calculations by Dance,[18,35−38] Norskov and co-workers,[39−41] Blochl and co-workers,[42] Case, Lovell, and Noodleman,[43,44] and Ahlrichs[45] have used chemically complete or almost complete models for FeMo-co. Only five of these reports have included results about the hydrogen chemistry of FeMo-co,[39,41,42,44,45] and some have developed models that appear to me to be chemically improbable. Previous theoretical work has not probed the hydrogen chemistry of FeMo-co as completely as intended in this paper.

Because all of the biochemical evidence is pointing toward the Fe_4S_4 face under the α-70 residue (of *A. vinelandii*), and more specifically the atoms Fe2 and Fe6 (see Figure 1), as the binding domain for alkenes, their reduced intermediates, and nitrogen, this region of FeMo-co is the focus of the investigation reported here.

The results are organized around the following questions. (1) How are protons translocated from protein to FeMo-co in conjunction with electron addition to FeMo-co, and which atom of FeMo-co is the probable site of initial hydrogenation? This is addressed by examination of the protein structure, and by density functional calculations of the H^+ basicity of FeMo-co as electrons are added. (2) How are H atoms bound to the S atoms of FeMo-co? (3) How are H atoms bound to the Fe atoms of FeMo-co? (4) How can H atoms move around the binding sites of FeMo-co? (5) How does H_2 coordinate to FeMo-co, and how tightly is it bound? (6) How can H_2 be generated on FeMo-co? (7) What are the possibilities for H atoms and H_2 molecules bound to FeMo-co, and how do H atoms affect the reaction profiles for association/dissociation of H_2? (8) What H/H_2 exchange processes can occur at FeMo-co? From these results, the general principles for the hydrogen coordination chemistry of FeMo-co are extracted, and hypotheses developed for the next stages of the investigation incorporating substrates (N_2, C_2H_2) and exogenous inhibitors (CO).

Methodology

The model **1** used for FeMo-co retains the native coordination of all influential atoms.

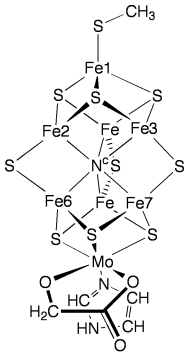

1

Density functional calculations used Delley's program DMol,[46] which uses double numerical basis sets with polarization functions.[47] The calculations are all-electron (477 electrons for the unligated cluster) and spin-unrestricted, and use the blyp functional with a fine computational grid. During geometry optimizations, the electron configurations were in general uncontrolled, and (through use of Fermi smearing) allowed to adopt the orbital occupation and molecular spin that yield lowest energy. In most cases, alternative spin states were also investigated, and, where optimized geometry varied with spin, each geometry was also optimized with the alternate spin. In this way, alternative electronic states for some structures were revealed. The electronic structure of **1** has ca. 20 filled orbitals within 2 eV of the HOMO, and a HOMO−LUMO gap which is generally about 0.4 eV, and geometrically similar structures can occur in different electronic and spin states with similar energies. Some of these alternatives are reported in this paper. All spin values reported are FeMo-co molecular spin.

Structures reported as local minima were checked through lack of gradient for further change, instead of frequency calculations, which can be dubious for large loose clusters such as FeMo-co with multiple very low frequency modes. This strategy is consistent with the objective of locating and mapping the relatively flat domains of the hypersurface of hydrogenated FeMo-co, domains which will be most relevant to its reactivity and mechanism.

Reaction processes have been investigated with manual interpolation of geometry and iterative evaluations of energy and energy gradient. The general procedure[48] was to observe

(24) Jessop, P. G.; Morris, R. H. *Coord. Chem. Rev.* **1992**, *121*, 155−284. Heinekey, D. M.; Oldham, W. J. *Chem. Rev.* **1993**, *93*, 913−926. Crabtree, R. H. *Angew. Chem., Int. Ed. Engl.* **1993**, *32*, 789−805.
(25) Maseras, F.; Lledos, A.; Clot, E.; Eisenstein, O. *Chem. Rev.* **2000**, *100*, 601−636.
(26) Kubas, G. J. *Metal Dihydrogen and -Bond Complexes*; Kluwer Academic/Plenum: New York, 2001.
(27) Siegbahn, P. E. M.; Westerberg, J.; Svensson, M.; Crabtree, R. H. *J. Phys. Chem. B* **1998**, *102*, 1615−1623.
(28) Szilagyi, R. K.; Musaev, D. G.; Morokuma, K. *THEOCHEM* **2000**, *506*, 131−146.
(29) Szilagyi, R. K.; Musaev, D. G.; Morokuma, K. *Inorg. Chem.* **2001**, *40*, 766−775. Durrant, M. C. *Inorg. Chem. Commun.* **2001**, *4*, 60−62. Reiher, M.; Hess, B. A. *Chem.-Eur. J.* **2002**, *8*, 5332−5339.
(30) Durrant, M. C. *Biochem. J.* **2001**, *355*, 569−576.
(31) Durrant, M. C. *Biochemistry* **2002**, *41*, 12934−12945.
(32) Durrant, M. C. *Biochemistry* **2002**, *41*, 12946−13955.
(33) Stavrev, K. K.; Zerner, M. C. *Int. J. Quantum Chem.* **1998**, *70*, 1159−1168. Helleren, C. A.; Henderson, R. A.; Leigh, G. J. *Dalton Trans.* **1999**, 1213−1220. Sellmann, D. *New J. Chem.* **1997**, *21*, 681−689. Lehnert, A.; Wiesler, B. E.; Tuczek, F.; Hennige, A.; Sellmann, D. *J. Am. Chem. Soc.* **1997**, *119*, 8869−8878. Sellmann, D.; Fursatt, A. *Angew. Chem., Int. Ed.* **1999**, *38*, 2023−2026. Reiher, M.; Salomon, O.; Sellmann, D.; Hess, B. A. *Chem.-Eur. J.* **2001**, *7*, 5195−5202. Sellmann, D.; Hille, A.; Heinemann, F. W.; Moll, M.; Reiher, M.; Hess, B. A.; Bauer, W. *Chem.-Eur. J.* **2004**, *10*, 4214−4224. Barriere, F. *Coord. Chem. Rev.* **2002**, *236*, 71−89.
(34) Seefeldt, L. C.; Dance, I. G.; Dean, D. R. *Biochemistry* **2004**, *43*, 1401−1409.
(35) Dance, I. G. *Aust. J. Chem.* **1994**, *47*, 979−990.
(36) Dance, I. G. *J. Chem. Soc., Chem. Commun.* **1997**, 165−166.
(37) Dance, I. *J. Chem. Soc., Chem. Commun.* **1998**, 523−530.
(38) Dance, I. *Chem. Commun.* **2003**, 324−325.
(39) Rod, T. H.; Norskov, J. K. *J. Am. Chem. Soc.* **2000**, *122*, 12751−12763.
(40) Hinnemann, B.; Norskov, J. K. *J. Am. Chem. Soc.* **2003**, *125*, 1466−1467.
(41) Hinnemann, B.; Norskov, J. K. *J. Am. Chem. Soc.* **2004**, *126*, 3920−3927.
(42) Schimpl, J.; Petrilli, H. M.; Blochl, P. E. *J. Am. Chem. Soc.* **2003**, *125*, 15772−15778.
(43) Lovell, T.; Li, J.; Liu, T.; Case, D. A.; Noodleman, L. *J. Am. Chem. Soc.* **2001**, *123*, 12392−12410. Lovell, T.; Li, J.; Case, D. A.; Noodleman, L. *J. Biol. Inorg. Chem.* **2002**, *7*, 735−749. Noodleman, L.; Lovell, T.; Liu, T.; F., H.; Torres, R. A. *Curr. Opin. Chem. Biol.* **2002**, *6*, 259−273. Lovell, T.; Liu, T.; Case, D. A.; Noodleman, L. *J. Am. Chem. Soc.* **2003**, *125*, 8377−8383.
(44) Lovell, T.; Li, J.; Case, D. A.; Noodleman, L. *J. Am. Chem. Soc.* **2002**, *124*, 4546−4547.
(45) Huniar, U.; Ahlrichs, R.; Coucouvanis, D. *J. Am. Chem. Soc.* **2004**, *126*, 2588−2601.
(46) Delley, B. *J. Chem. Phys.* **1990**, *92*, 508−517. Delley, B. In *Modern density functional theory: a tool for chemistry*; Seminario, J. M., Politzer, P., Eds.; Elsevier: Amsterdam, 1995; Vol. 2, pp 221−254. Delley, B. *J. Chem. Phys.* **2000**, *113*, 7756−7764.
(47) DMol3 version MS 3.0 2003. www.accelrys.com/mstudio/ms_modeling/dmol3.html.
(48) Harris, H.; Fisher, K. J.; Dance, I. G. *Inorg. Chem.* **2000**, *40*, 6972−6982.

the initial changes in geometry and gradient during small-step energy minimizations from an intermediate geometry, and then to use this information to build a new intermediate geometry expected to be just on the other side of the barrier. This cycle was iterated to find the lowest energy structure that will optimize to reactants or products when nudged. Care has been taken to follow the surface of one electronic state for each reaction profile, but because FeMo-co and its derivatives have close-lying electronic states it is not always certain that the one electronic state is being followed: this uncertainty was reduced by using optimizations from the transition state as the reactant and product states, and by monitoring the behavior of the self-consistent-field calculations because they can signal clandestine changes in electronic state. Saddle points have been located for transitions, but, in view of the multiple geometrical variables that will become apparent, there may be uncertainty that the best saddle point has been found, and so the barrier energies could be less than the values reported. Transition states for postulated key mechanistic steps are being investigated with quadratic synchronous transit methods, to be published separately.

Validation of Methods

This DMol density functional methodology has been validated against a variety of metal sulfide clusters and related compounds[37,49] and has been applied extensively to the FeMo-co cluster and its properties.[18,36,38,50] It is important to understand its accuracy in calculations of geometrical structure, energy, and spin/electronic states. Detailed results from many validation calculations are presented in the Supporting Information and are summarized here. Comparison of the geometry of FeMo-co in crystal structure 1M1N with that calculated with the present methodology (for $S = {}^3/_2$ and $S = {}^1/_2$ states) gives good overall agreement (Table S1): calculated mean Fe−S distances in the various classes are 0.02−0.06 Å longer than the crystal structure; the calculated mean Fe−N^c distance is 0.05 Å longer; the mean calculated Mo−(μ_3-S) distance is 0.08 Å longer; calculated mean Fe--Fe distances of the two types are 0.02 and 0.07 Å longer than observed. Thus, this methodology is just slightly under-binding, with bond length inaccuracies of ca. 0.05 Å. It is important to recognize that FeMo-co is a plastic cluster in which interatomic distances can vary appreciably with relatively small energy penalty. This plasticity of FeMo-co, particularly with bound substrates, will be evident in results presented below.

Two well-characterized coordination complexes relevant to the present systems are $Fe(H)_2(H_2)(PEtPh_2)_3$[51] and $Fe(H)_2(\eta^1\text{-}N_2)(PEtPh_2)_3$.[51] These structures (in full) have been optimized with the current DMol methods, and compared with the crystal structures (Tables S2, S3). For $Fe(H)_2(H_2)(PEtPh_2)_3$ (neutron diffraction structure), the calculated Fe−H distances are 0.01−0.07 Å longer than experimental, H−H is 0.03 longer than experimental, and the various H−Fe−H angles are within 1° of experimental. For $Fe(H)_2(N_2)(PEtPh_2)_3$, calculated distances within the $Fe(H)_2(N_2)$ set are within 0.01 Å of experimental values, and angles agree within 4°. In all Fe−phosphine complexes, the Fe−P distances are calculated to be ca. 0.1 Å longer than measured, but this is not an issue for the chemistry of FeMo-co. Complexes $[Fe(PMe_3)_4H_3]^+$ and $[Fe(PMe_3)_4H(H_2)]^+$ (and homologues) have been characterized in crystals and in solution.[52] My calculations reproduce the relevant local minima and calculate a potential energy difference between these structures of 5 kcal mol^{-1} (in favor of $[Fe(PMe_3)_4H(H_2)]^+$): experimentally, the enthalpy difference between them is estimated to be almost zero in solution. The compound $[PhB(CH_2PPr^i)_3]Fe(H)(PMe_3)$ has distorted five coordination and is $S = 1$. I have optimized the $S = 0$ and $S = 1$ states of this compound and show (Table S4) that the $S = 1$ state reproduces the angular distortions while the $S = 0$ state does not. The unusual compound $(P^iPr_3)_2(H)_2Ru(\mu\text{-}H)_3Ru(H)(P^iPr_3)_2$ contains a triple bridge of H atoms, and terminal H atoms, on two different Ru atoms, one seven-coordinate, one six-coordinate.[53] The calculated Ru−H distances track the experimental variations in the different types of Ru−H bond (Table S5).

My calculated internal energy change for $N_2 + 3H_2 \rightarrow 2NH_3$ is −14.8 kcal mol^{-1}; Siegbahn[27] states without reference that the experimental value is −17.8 kcal mol^{-1}. My calculated $\Delta H_f(NH_3)$ is −12.6 kcal mol^{-1}; experimental −11.9 kcal mol^{-1}.[54,55]

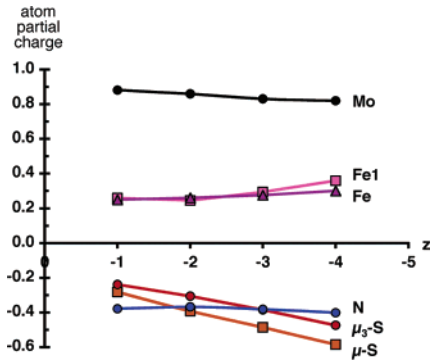

Figure 2. Calculated average partial charges for the different types of cluster atoms according to the total charge z of $\mathbf{1}^z$.

Pathways for H Addition

A first step is introduction of a proton to the active site, in conjunction with the introduction of an electron. The basic concept is that a proton is transferred from a close proton donor group (protein or water) to an S atom of FeMo-co, which then transfers a hydrogen atom to the substrate or intermediate. I do not exclude any possibility of direct transfer of proton from surrounds to substrate, but, as will be demonstrated, the S atoms of FeMo-co provide energetically favorable mediators for the hydrogenation events. Addition of electrons to FeMo-co increases negative charge most strongly on the S atoms, as illustrated by the calculated partial charges[56] on atoms of different types for model **1** at four different redox levels, as shown in Figure 2. On reduction of FeMo-co, the partial charge on N^c is unaffected and the charge on Mo changes negligibly, while the S atoms become increasingly negative. There is a small

(49) Dance, I. G.; Fisher, K. J. *Prog. Inorg. Chem.* **1994**, *41*, 637−803. Dance, I. G. In *Transition Metal Sulfur Chemistry: Biological and Industrial Significance*; Stiefel, E. I., Matsumoto, K., Eds.; American Chemical Society: Washington, DC, 1996; Vol. 653, pp 135−152.
(50) Dance, I. G. *J. Biol. Inorg. Chem.* **1996**, *1*, 581−586.
(51) Van Der Sluys, L. S.; Eckert, J.; Eisenstein, O.; Hall, J. H.; Huffman, J. C.; Jackson, S. A.; Koetzle, T. F.; Kubas, G. J.; Vergamini, P. J.; Caulton, K. G. *J. Am. Chem. Soc.* **1990**, *112*, 4831−4841.
(52) Gusev, D. G.; Hubener, R.; Burger, P.; Orama, O.; Berke, H. *J. Am. Chem. Soc.* **1997**, *119*, 3716−3731.
(53) Abdur-Rashid, K.; Gusev, D. G.; Lough, A. J.; Morris, R. H. *Organometallics* **2000**, *19*, 1652−1660.
(54) Chase, M. W. *J. Phys. Chem. Ref. Data* **1998**, *9*, 1−1951.
(55) http://webbook.nist.gov/chemistry.
(56) Atom charges are expressed as the averages of the Mulliken, Hirshfeld, and ESP (fitted to the electrostatic potential) calculated values.

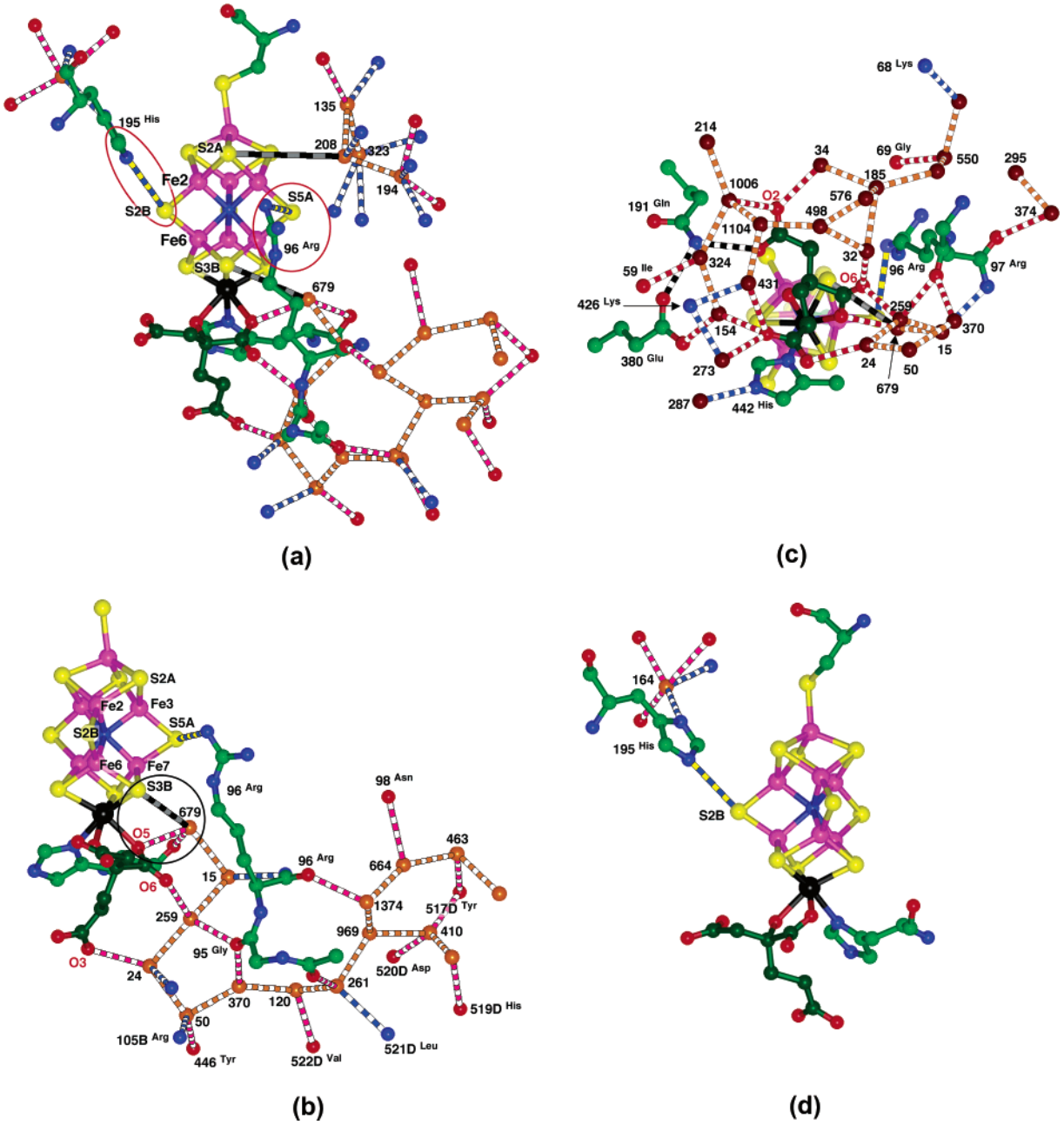

Figure 3. Proton donors to relevant S atoms of FeMo-co, and connected hydrogen-bond chains. C atoms of homocitrate are darker green; water molecules (brown) are labeled with numbers from structure 1M1N; residue N,O atoms are blue, red, respectively. N−H···S hydrogen bonds from α-195^{His} and α-96^{Arg} to the μ-S atoms S2B and S5A are marked with blue/yellow stripes and red enclosures, and the potential hydrogen bonds from water molecules 208 and 679 to S2A and S3B respectively are marked with black/gray stripes: the S3B--HOH679 distance is 4.01; the S2A--HOH208 distance is 5.27. Water−water hydrogen bonds are orange/white; water--N hydrogen bonds are blue/white; water--O hydrogen bonds are red/white; peptide−peptide hydrogen bonds are black/white. (a) Standard front view, including the cluster of hydrogen bonds involving water molecules 208, 135, 323, 194, the S2B···α-195^{His} hydrogen bond, and the connection of S3B to water 679 and beyond. (b) Details of the chain of hydrogen-bonded water molecules extending from water 679, and the residues with which they are hydrogen bonded. The three involved O atoms of homocitrate are labeled in red. Note that three of the first four water molecules in the chain (679, 15, 259, 24) have hydrogen bonds with homocitrate. The black enclosure emphasizes alternative hydrogen-bonding possibilities from water 679 to homocitrate O5 or to S3B, discussed in the text. (c) View from underneath FeMo-co showing another hydrogen-bond chain extending from water 679 to water 259, O6 of homocitrate, water 32, and then through a variety of water molecules and O2 of homocitrate to residues α-380^{Glu} and α-191^{Gln}. (d) The surrounds of water 164, in relation to 195^{His} and S2B.

and counter-intuitive shift of negative charge from Fe to S as FeMo-co is reduced; that is, Fe atoms become more positive as FeMo-co is reduced, so that S atoms can become even more negative.

Accordingly, a fundamental mechanistic concept is that electron transfer to FeMo-co increases the basicity of S atoms toward nearby proton donors, and that the H atoms added in each e^-/H^+ cycle of nitrogenase are most probably located on S atoms, which become HS^- ligands. The probability of proton binding to the S atoms of FeMo-co is widely accepted.[27,32,35,36]

Proton Delivery Agents

Given that substrates probably bind to Fe6 and/or Fe2, over the Fe2,S2A,Fe3,S5A,Fe7,S3B,Fe6,S2B face (Figure 1), what are the potential proton donors? The relevant parts of the surrounds are illustrated in Figure 3. A histidine residue (α-

195 in *Azotobacter vinelandii* Av, 1M1N; α-194 in *Klebsiella pneumoniae* Kp, 1QGU; hereafter residue numbering is that of Av) is within hydrogen-bonding distance of S2B, and when protonated at Nϵ can function as proton donor to S2B. A terminal NH group of α-96^{Arg} can similarly hydrogen bond and proton donate to S5A (Figure 3a,b): in the crystal structure of Kp MoFe protein, the side chain of this residue is displaced, and this interaction with S5A is very long. There are no water molecules that could function as proton donors to these doubly bridging S2B or S5A atoms, but there are water molecules to be considered as proton donors to the triply bridging S2A and S3B atoms, and these interactions are marked with black and gray stripes in Figure 3. The more significant is between S3B and water 679, because this water molecule is the terminus of several chains of hydrogen-bonded water molecules (Figure 3a–c). One water chain involves putative hydrogen bonds with three of the carboxylate O atoms of homocitrate (O3, O5, O6) as well as the carbonyl O atoms of α-96^{Arg}, α-95^{Gly}, α-94^{Ala}, and a number of other residues. This water network is more elaborate than the section shown in Figure 3b: it has been described previously as the "water pool"[2,28] or "interstitial channel".[30] The second water chain (Figure 3c) is from water 679 to water 259, O6 of homocitrate, water 32, and then through a variety of water molecules and O2 of homocitrate to residues α-380^{Glu} and α-191^{Gln}. These two water chains involve hydrogen bonds with five of the oxygen atoms of homocitrate, consistent with the strict requirement for homocitrate.[57] It is proposed that protons are passed along one or both of these chains to water 679, and then to the side of S3B that is opposite to Fe6. The importance of water 679 is supported by its conserved position in the higher resolution crystal structures of the FeMo protein (values in parentheses are the corresponding S--O distances (Å) for each of the FeMo cofactors): 1M1N (4.01, 4.04, 4.03, 4.04); 1QGU (4.05, 4.05); 1G20 (4.16); 1QH1 (4.02, 4.06); 1H1L, containing citrate in place of homocitrate (3.81, 3.78). This S3B to O distance of 4.0 Å in 1M1N is longer than the normal hydrogen-bond distance (ca. 3.2 Å) for water to cluster sulfide, but, as demonstrated in the results to follow, there is movement of S3B toward water 679, facilitating the proton transfer.

The other potential proton donor water molecule is 208, directed toward S2A on the side opposite to Fe2. The O(208)--S2A distance is long (5.27 Å), which appears to preclude this as a proton transfer pathway, but two factors ameliorate this concern. One is that S2A can move in the direction of water-208, as described below, and the other is that the local net of other water molecules (135, 323, 194) and surrounding residues appears to involve distorted hydrogen bonds, suggesting that the position of water 208 in the active protein is variable and possibly more favorable. However, the proton donor pathway via water 679 to S3B is much more promising than that via water 208 to S2A.

If Nϵ of α-195^{His} is to function as proton donor to S2B, there is a question about the pathway for proton supply to this residue. This section of the protein is largely devoid of water molecules. As shown in Figure 3d, there is a water molecule (164) hydrogen bonded to Nδ of α-195^{His} and to other surrounding residues, and this water molecule is present in the reported crystal structure of the Kp protein,[3] but a proton-transfer pathway is not obvious.

Results

The objective of this density functional investigation is to explore and map the geometry-energy hypersurface for hydrogen atoms and molecules bonded to FeMo-co, as relevant to the mechanism of nitrogenase, and to discern important principles. This has been done by constructing many possible models and observing the course (geometry, energy, and gradient) of their energy minimizations, and, through iteration, locating key local energy wells and saddle points between them. It is important to recognize that FeMo-co, particularly when ligated at the central Fe and S atoms, is quite plastic and that there are many metrical variables. Parts of the energy surface are relatively flat and therefore are possibly significant for enzyme mechanism. The multiple variables and the flatness of parts of the energy surface mean that gradient directed optimizations need to be monitored carefully, and a large amount of manual modification of variables has been used in mapping the energy surfaces and finding both local minima and transition states.

Hydrogenated FeMo-co, like FeMo-co itself and coordinated by other ligands, is characterized by close-lying electronic and spin states, and this property has been included by checking alternative spin and electronic states of key structures. Energy differences of ca. 3 kcal mol^{-1} and occasionally up to 10 kcal mol^{-1} have been observed for different electronic states of very similar geometries. In investigations of the energy changes and barriers for transformations, care has been taken to ensure that the same electronic state prevails. Only those results that illustrate well the main principles of the coordination chemistry of FeMo-co with hydrogen are presented.

Energies are referenced in two ways: for single structures **1**−H_x, the energies (symbol E, kcal mol^{-1}) are quoted relative to $[E(\mathbf{1}) + (x/2)E(H_2)]$; for transformations the energies of reactant, transition state, and product are referenced to either the reactant or the product energies as appropriate. It is recognized that the chemical potential of H (as $e^- + H^+$) in the enzyme may differ appreciably from that calculated from $^1/_2H_2$ in the gas phase,[42] but because the chemical potential varies with H location and is unknown, while the H_2(g) reference is unambiguous and transportable, the H_2(g) reference is adopted here.

(1) How Are H Atoms Bound to the S Atoms of FeMo-co? I have explored the potential energy surfaces for FeMo-co with a hydrogen atom associated with one of the three relevant types of S atom, S3B, S2A, or S2B.

H on μ_3-S. When the μ_3-S atoms (S2A, S3B) form S−H bonds, it is generally found that there is concomitant weakening of S−Fe bonds. That is, when μ_3-S becomes μ_3-SH, the S atom is four-coordinate, and can change in various ways with weakening of one S−Fe (or S−Mo) bond, toward μ_2-SH. Consequently, quite different geometrical structures can be energetically similar and accessible.

Six different conformations of H bonded to a μ_3-S atom of FeMo-co occur and are charted in Figure 4 with the conformer labels used throughout this paper. Because Fe2 and Fe6 are targeted in probable mechanisms, the labels of the conformers at S2A are referenced to Fe2, and those at S3B are similarly

(57) Imperial, J.; Hoover, T. R.; Madden, M. S.; Ludden, P. W.; Shah, V. K. *Biochemistry* **1989**, *28*, 7796−7799. Madden, M. S.; Kindon, N. D.; Ludden, P. W.; Shah, V. K. *Proc. Natl. Acad. Sci. U.S.A.* **1990**, *87*, 6517−6521.

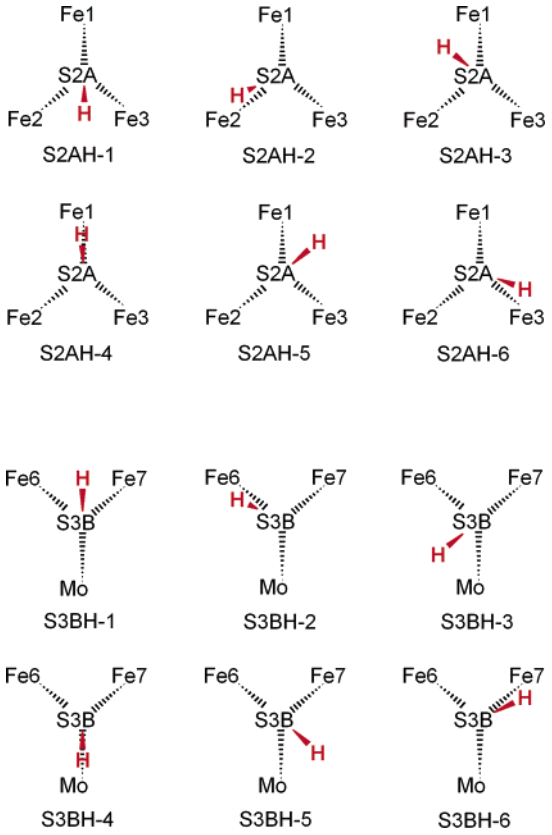

Figure 4. Chart of the six conformation types for an S−H bond at the μ_3-S atoms S2A and S3B. The labels are referenced to Fe2 for S2A, and to Fe6 for S3B.

referenced to Fe6. Conformations **SH-2** and **SH-6** are directed near S−Fe bonds and commonly occur as S−H−Fe bridges (and are generically named as bridging isomers); conformations **SH-3** and **SH-5** are opposite Fe−S bonds and are named opposite isomers; conformation **SH-1**, a transition between **SH-2** and **SH-6**, is non-pyramidal at S; conformation **SH-4** is pyramidal μ_3-SH and is the transition between **SH-3** and **SH-5**. Conformations **SH-2** and **SH-6** (and **SH-3**, **SH-5**) are equivalent in terms of immediate bonding to FeMo-co but are differentiated by the surrounding protein and in mechanistic possibilities.

Structures have been optimized for the six conformations of H at S3B and at S2A, with spin states $S = 0$ and $S = 1$, and a representative structure for each conformation is depicted in Figure 5 (in which only the immediate atoms are pictured). Elongated Fe−S or Mo−S bonds are shown with stripes, and lengths are marked. Additional structures for alternative spin/electronic states for each conformer show energy variations of ca. 5 kcal mol^{-1} according to electronic state. The important results for these structures are: (1) stable, tight Fe−H−S bridges occur, with Fe--S ca. 2.65 Å; (2) the Fe−S bonds opposite to S−H (in conformations **S3BH-3**, **S3BH-5**, **S2AH-3**, **S2AH-5**) are elongated, as is the Mo−S3B bond in **S3BH-1**; (3) the energies of the bridged conformations (**S3BH-2**, **S3BH-6**, **S2AH-2**, **S2AH-6**) and the opposite conformations (**S3BH-3**, **S3BH-5**, **S2AH-3**, **S2AH-5**) range over less than 7 kcal mol^{-1}; (4) structures **S3BH-1**, **S3BH-4**, and **S2AH-1**, **S2AH-4**, indicate that the barrier for inversion of H from one side of S3B or S2A to the other, including changes in two Fe−S bonds, is 10−15 kcal mol^{-1}. The energy surfaces for H bound to S3B or S2A are relatively flat, and an H atom can move around the region of the adjacent Fe (Mo) atoms and the Fe−S bonds: structure **S3BH-3** in one electronic state (not shown) undergoes barrierless transformation to **S3BH-2**.

The S2A−H structures and the S3B−H structures differ notably in the Fe−S distances opposite to SH (in structures **SH-3**, **SH-5**): at S2A these Fe--S distances range from 3.2 to 3.6 Å and are very weak interactions, while at S3B these distances (ca. 2.65 Å) are but partially weakened bonds. I believe that this difference occurs because S2A is bound to Fe1, which is

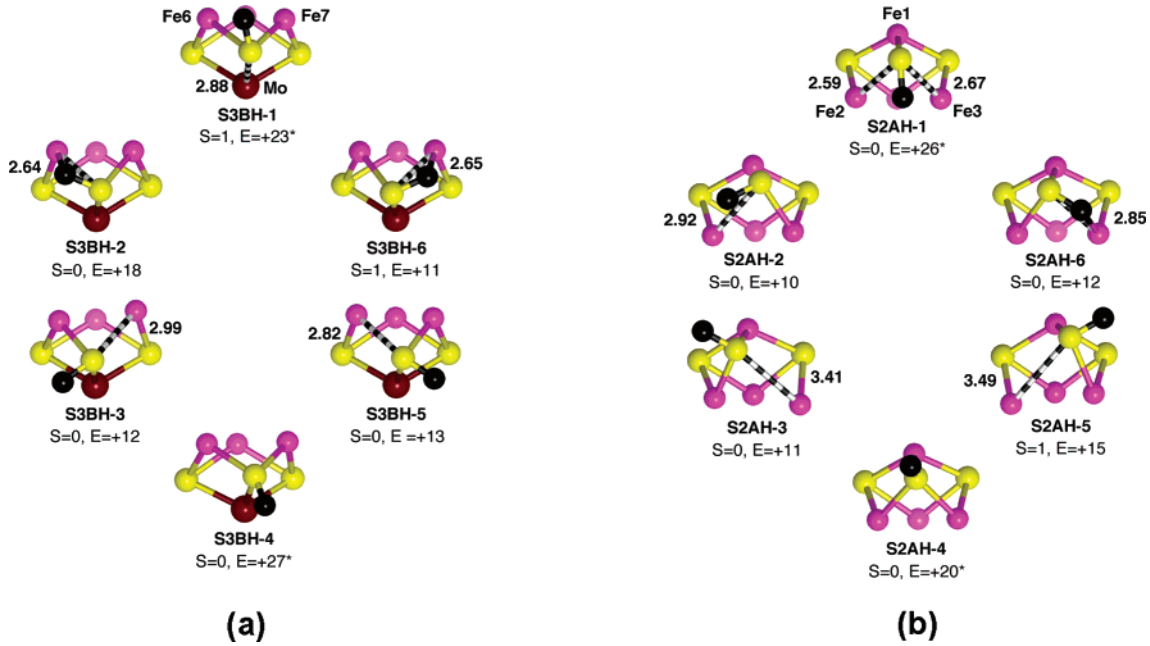

Figure 5. Chart of representative structures on the potential energy surface for one H atom bound to (a) S3B or (b) S2A of FeMo-co: Mo is brown, H is enlarged black, and the local atoms only are drawn. * indicates that the structure is not a local energy well. Spin states and energies (kcal mol^{-1}) relative to [E(**1**) + $^1/_2E(H_2)$] are marked, as are the lengths (Å) of elongated bonds which are drawn striped. In the Fe6−H−S3B bridges (**S3BH-2**, **S3BH-6**), the distances are Fe−H 2.0 and S−H 1.4 Å, and in the Fe2−H−S2A bridges (**S2AH-2**, **S2AH-6**), the Fe−H distances are 2.2−2.4 Å.

four-coordinate and tetrahedral, permitting the angular distortion at Fe1 which occurs when distances between S2A and other Fe atoms are increased, while S3B is bound to Mo, which is six-coordinate and therefore has a larger energy penalty for angular distortion. Additional differentiations between the Mo and Fe ends of FeMo-co are described in section 12; this indirect geometrical influence of Mo in FeMo-co is probably mechanistically significant in a number of ways.

Note that conformation **S3BH-5** places H in the direction that S3B would receive a proton from water 679 (Figure 3a) and has S3B moved toward this proton donor. Further, conformations **SH-1**, **SH-2**, and **SH-3** direct the H atom toward substrates bound at Fe6 or Fe2. These portentous properties are discussed near the end of this paper.

H on μ-S. A hydrogen atom bonded to the doubly bridging atom S2B generates a μ-SH ligand with pyramidal stereochemistry at S, and two almost equivalent conformations that are endo or exo to a specific Fe_4S_4 face of FeMo-co. At S2B the relevant conformation that is endo to the Fe2,Fe3,Fe6,Fe7 face is shown in Figure 6 as **S2BH-1**. The transition state for inversion of S2B-H is structure **S2BH-3** (planar at S2B, see Figure 6), with a barrier of ca. 20 kcal mol^{-1}. The H atom on S2B can move from the optimum pyramidal conformation, as illustrated in **S2BH-2**, which is ca. 10 kcal mol^{-1} above the minimum. An important function of S2B is to interact with 195^{His} as shown in Figure 3d, and conformation **S2BH-4** has the H directed toward Nϵ of this residue, with an energy penalty of ca. 14 kcal mol^{-1}.

(2) How Are H Atoms Bound to the Central Fe Atoms of FeMo-co? Geometrical isomers exist for coordination of H to a central Fe atom of FeMo-co. In the exo isomers (**3**, **4**), the Fe−H bond is close to collinear with the Fe−N^c bond, while in the endo isomer (**2**), the Fe−H bond is approximately perpendicular to Fe−N^c and directed into one of the Fe_4S_4 faces. Endo-Fe−H coordination is square-pyramidal at Fe, approaching-square planar if Fe−N^c is weakened. In the exo-Fe−H isomer, the coordination stereochemistry of Fe depends on the length of the Fe−N^c bond, which in general can vary from 2.0 Å to more than 3.0 Å. The Fe coordination is trigonal bipyramidal in exo-Fe−H structures with shorter Fe−N^c (**3**), and tetrahedral when Fe−N^c is longer (**4**). The key differentiating descriptors of Fe−H coordination are the Fe−N^c distance and the N^c−Fe−H angle. The S−Fe−S angles at Fe also differ because the exo coordination is approximately trigonal while the endo coordination is approximately square.

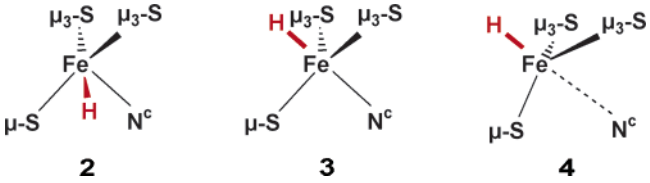

The lowest energy isomers at Fe2 and Fe6 are shown in Figure 7. The main results are (1) exo-Fe−H coordination is ca. 15 kcal mol^{-1} more stable than endo-Fe−H, (2) Fe−N^c is longer for exo-Fe−H than for endo-Fe−H, and (3) in endo-Fe−H coordination the μ-S atom is folded back (by ca. 0.5 Å) so that the H atom can be accommodated within the (μ-S)-Fe−(μ_3-S) angle of ca. 145°. Interconversion of the exo and endo isomers involves only angular variations, and there is a smooth

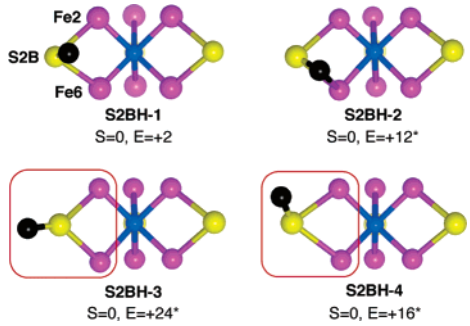

Figure 6. Structures relevant to the potential energy surface of a H atom bound to S2B, drawn as only the central (μ_6-N)(μ-S)$_2$(μ-SH)Fe$_6$ atoms of FeMo-co. Energies (kcal mol^{-1}) are relative to [E(**1**) + $^1/_2E$(H$_2$)]. Only **S2BH-1** is an energy minimum. In **S2BH-3** and **S2BH-4**, the atoms enclosed in red are coplanar. In **S2BH-2**, H−Fe6 = 2.4 Å.

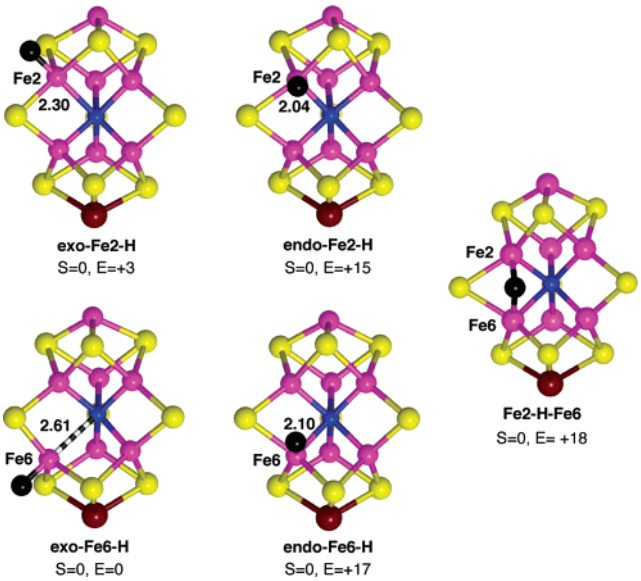

Figure 7. The exo and endo isomers for H coordinated to Fe2 or Fe6 of FeMo-co, and the Fe2−H−Fe6 bridging structure. The distances (Å) marked are N^c−Fe. Energies (kcal mol^{-1}) are relative to [E(**1**) + $^1/_2E$(H$_2$)].

arc of coordination positions between the two isomers. The transition state for this interconversion is closer to the endo isomer, and about 3 kcal mol^{-1} above the endo isomer: progression to the exo isomer involves movement of Fe away from N^c followed by contraction of the (μ-S)-Fe−(μ_3-S) angle as the N^c−Fe−H angle increases.

A single H atom can also bridge a pair of Fe atoms from different ends of FeMo-co, such as Fe2 and Fe6, along the prism edges of the central Fe_6 set. This bridging H atom is close to the endo coordination position of both Fe atoms involved, and this structure **Fe2−H−Fe6** (see Figure 7) is characterized by approximately equal Fe−H distances, μ-S folded back, and Fe−Fe shortened by ca. 0.15 Å. The energy of the Fe2−H−Fe6 bridging isomer is within 3 kcal mol^{-1} of the related endo Fe−H isomers and is located in a very shallow energy well. The energy profile for the interconversion of the bridge and the separate endo-Fe−H structures is remarkably flat, with all barriers for transfer of H from one Fe to the other via the bridge calculated to be <4 kcal mol^{-1} (Figure S1). Further, because the endo-Fe−H ⟹ exo-Fe−H barriers are also small, translocation of an H atom from the endo position on one Fe to exo-H on the other is predicted to be a facile process for FeMo-co.

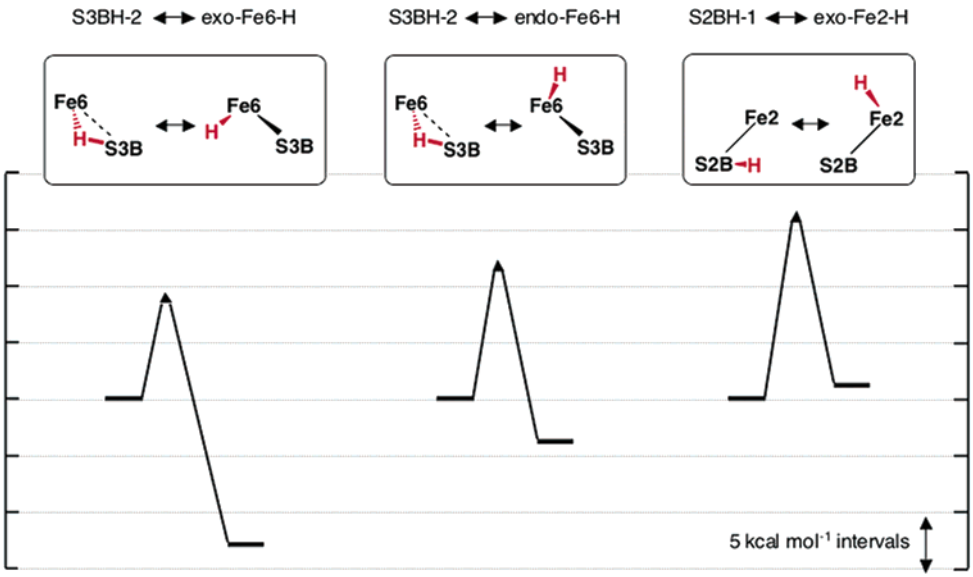

Figure 8. Reaction energy profiles for H transfer between S3BH-2 and exo-Fe6−H, between S3BH-2 and endo-Fe6−H, and between S2BH-1 and exo-Fe2−H (all $S = 0$).

Fe−H−Fe bridges involving the triangle edges (Fe2−H−Fe3 or Fe6−H−Fe7) or across a diagonal of the Fe_6 core (Fe2−H−Fe7 or Fe6−H−Fe3) are not stable and transform to other nonbridging Fe−H structures.

What are the polarities of the Fe−H and S−H bonds described above? Calculated partial charges and bond polarizations are $S^{-0.4}$−$H^{+0.1}$ for terminal S2BH and S3BH, $S^{-0.5}$−$H^{+0.1}$−$Fe^{+0.3}$ for bridging S3BH-2, $Fe^{+0.3}$−$H^{-0.1}$ for Fe−H, and $Fe^{+0.2}$−$H^{-0.1}$−$Fe^{+0.2}$ for the Fe2−H−Fe6 bridge. Because bound hydrogens vary in charge only between +0.1 and −0.1, they are described as H atoms.

(3) How Can H Atoms Move between the S and Fe Binding Sites of FeMo-co? Reaction profiles have been calculated for three H transfer processes, (a) between S3BH-2 and exo-Fe6−H, (b) between S3BH-2 and endo-Fe6−H, and (c) between S2BH-1 and exo-Fe2−H. The energies of the extremes and the transition state for each process are charted in Figure 8: for description of the geometrical changes for these processes, see Figures S2 and S3. The pathway from the bridging structure S3BH-2 to exo-Fe6−H is the most favorable, being exergonic by 13 kcal mol^{-1} with a barrier of 9 kcal mol^{-1}. There are changes in the distances Fe6−S3B (2.62 to 2.42 to 2.24 Å) and Fe6−N^c (2.05 to 2.14 to 2.61 Å) associated with this H transfer. The alternative transfer from S3BH-2 to the endo-Fe6−H has a slightly larger barrier of 12 kcal mol^{-1}, while for H transfer from S2B the barrier increases to 16 kcal mol^{-1}.

The conclusion at this point is that the most favored process is transfer of μ_3-S−H to exo-Fe−H. This extends the hypothesis that S3B is the H-entry site from the protein, by providing the pathway for that H atom to move to an Fe atom.

(4) Structures with More than One H Atom. Many structures are possible with two or more H atoms on Fe and S atoms, formed by combinations of the possibilities for single H atoms on Fe and/or S previously described in sections 1 and 2. The only combination that is not possible geometrically is endo-Fe2−H plus endo-Fe6−H, where the H atoms clash. Calculations show that one Fe_4S_4 face of FeMo-co can bind up to eight H atoms: these heavily hydrogenated structures are not relevant to the questions of mechanism, but they do demonstrate the versatility of FeMo-co in binding H atoms. Some of the possibilities investigated led to the formation of H_2, bound to or dissociated from FeMo-co, and these are described in subsequent sections.

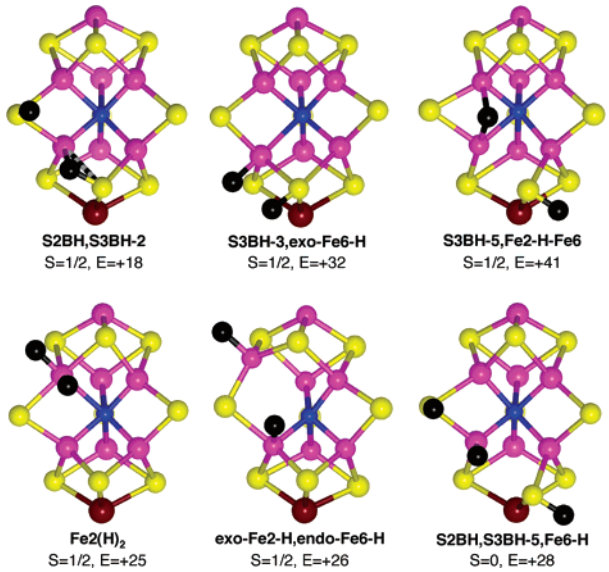

Figure 9. Six representative optimized structures with two or three H atoms bound to S and/or Fe atoms of FeMo-co: H atoms are black, extraneous atoms are omitted, and all pictures are in the standard orientation. Energies (kcal mol^{-1}) for FeMo-co + $(H)_n$ are relative to $[E(\mathbf{1}) + (n/2)E(H_2)]$. Fourteen additional optimized structures are described in Figure S4.

Twenty different structures with two or three H atoms on Fe and/or S have been optimized and are pictured in the Figure S4: Figure 9 presents a representative set of six of these structures. Structure names are composites of the names already introduced. Two or more H atoms can cause some additional distortion of the FeMo-co, particularly extension of Fe−N^c: for example, Fe2−N^c is 3.1 Å in **exo-Fe2−H,endo-Fe6−H**. In structures **Fe2(H)$_2$** and **Fe6(H)$_2$** (Figure S4), there is almost ideal octahedral coordination of Fe, with Fe−N^c distances ca. 2.45 Å. When the Fe6−S3B bond is severed, as in **S2BH,S3BH-5,Fe6−H** (Figure 9) the distinction between endo- and exo-Fe−H coordination is lost, and Fe6 has regular tetrahedral

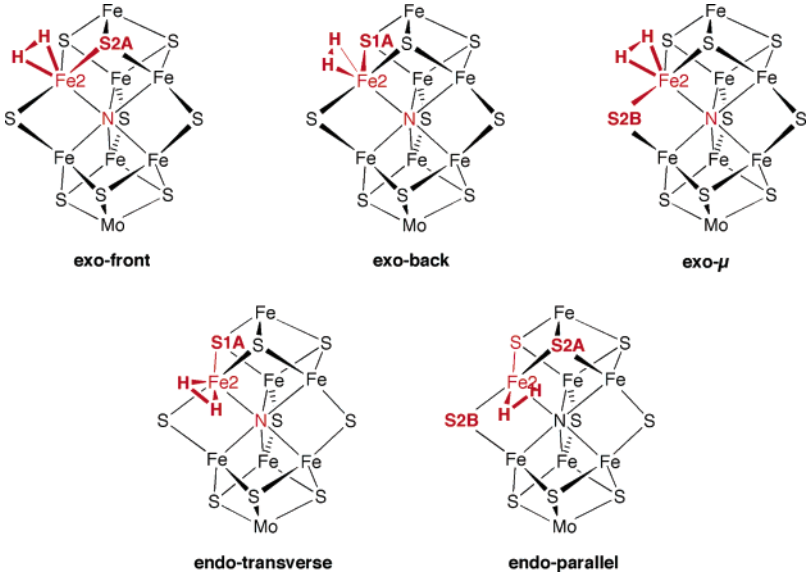

Figure 10. Isomers for η^2-coordination of H_2 to Fe, illustrated for Fe2. In each case, the red atoms are close to coplanar. In the exo-back conformer, the H−H bond is aligned with the Fe−μ_3-S bond behind the Fe_4S_4 reference face (S1A), while in the exo-front isomer, H−H is aligned with the Fe−μ_3-S bond in the Fe_4S_4 reference face (S2A).

coordination. In general, the lowest energy form of these structures is low spin ($S = 0$ or $^1/_2$). In broad terms, the relative energies of the structural types follow the principles already discerned, μ-SH is more stable than μ_3-SH, and exo-Fe−H is more stable than endo-Fe−H.

The 20 structures with two or three bound H atoms are candidates for the significant E_2 and E_3 states of the mechanistic cycle (Scheme 1). They are not the only possibilities. The ability of FeMo-co to bind H atoms could lead to additional feasible postulates for the distribution of H atoms over the Fe and S atoms. As mentioned, H_2 is calculated to form in a small number of the structures with multiple H atoms, which leads to the next question.

(5) How Does H_2 Coordinate to FeMo-co? Dihydrogen can be bound to a central Fe atom of FeMo-co in a number of ways, all with Fe-η^2-H_2 coordination. Exo and endo isomers exist, and because the ligand is diatomic, there is an additional conformational variable, which is rotation around the vector from Fe to the midpoint of H_2. The five isomers are illustrated for Fe2 in Figure 10 (analogous structures at Fe6 are named similarly): in each, the red atoms are close to coplanar. When H_2 is coordinated in the exo position, shallow local energy wells occur where the H−H bond is aligned with one of the three approximately trigonal Fe−S bonds. These conformers are labeled **exo-*μ*** when H−H is aligned with the Fe−(μ-S) bond, **exo-front** when H−H is aligned with the Fe−(μ_3-S) bond in the Fe_4S_4 reference face, and **exo-back** when the Fe−(μ_3-S) bond coplanar with Fe−H_2 is behind the Fe_4S_4 reference face. When H_2 is bound in the endo position, the μ-S atom is folded back and the Fe coordination is approximately square planar. Normally, H_2 is transverse to this plane (conformer **endo-transverse**), but when twisted through 90° there is the possibility, sometimes realized, of the **endo-parallel** conformer.

In addition to the isomerism of Figure 10, variations in the Fe−N^c length from 2.0 to 3.0 Å are found in energy-minimized structures. Six representatives of the 15 isomers (see Table S6) for H_2 bound to Fe2 or Fe6 are pictured in Figure 11, showing variations in Fe−N^c distance and coordination stereochemistry

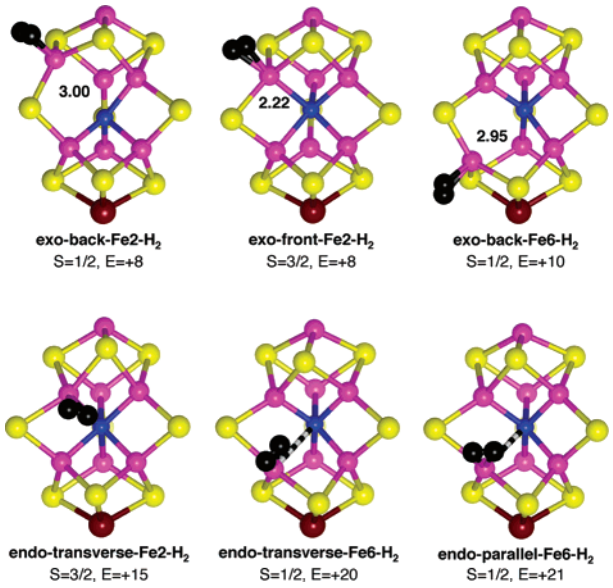

Figure 11. Comparative views of 6 of the 15 isomers for H_2 bound to Fe2 or Fe6. The upper structures illustrate the differences between exo-Fe−H_2 coordination with short (2.2 Å) and long (ca. 3.0 Å) Fe−N^c distances, which have trigonal bipyramidal and tetrahedral Fe coordination stereochemistry, respectively. The lower structures illustrate the difference between endo-Fe−H_2 coordination at Fe2, which has short Fe2−N^c = 2.30 Å and is square pyramidal at Fe, and at Fe6 which is square planar with longer Fe6−N^c (2.62, 2.48 Å).

at Fe. The relative energies of all isomers range from +1 to +21 kcal mol^{-1}.

What are the key properties of Fe−η^2-H_2 coordination? (1) Exo-Fe−H_2 is generally more stable by ca. 10 kcal mol^{-1} than endo-Fe−H_2. (2) Fe−H distances range from 1.62 to 1.85 Å, and the corresponding H−H distances range from 0.84 to 0.77 Å: slightly longer H−H and shorter Fe−H occur when Fe−N^c is long. (3) There are isomers for exo-Fe−H_2 with short (ca. 2.2 Å) and long (2.6−3.0 Å) Fe−N^c distance, resulting in trigonal bipyramidal and tetrahedral coordination stereochemistry respectively for Fe (see Figure 11). (4) There is negligible energy difference between the H_2-twist isomers for Fe−H_2, and

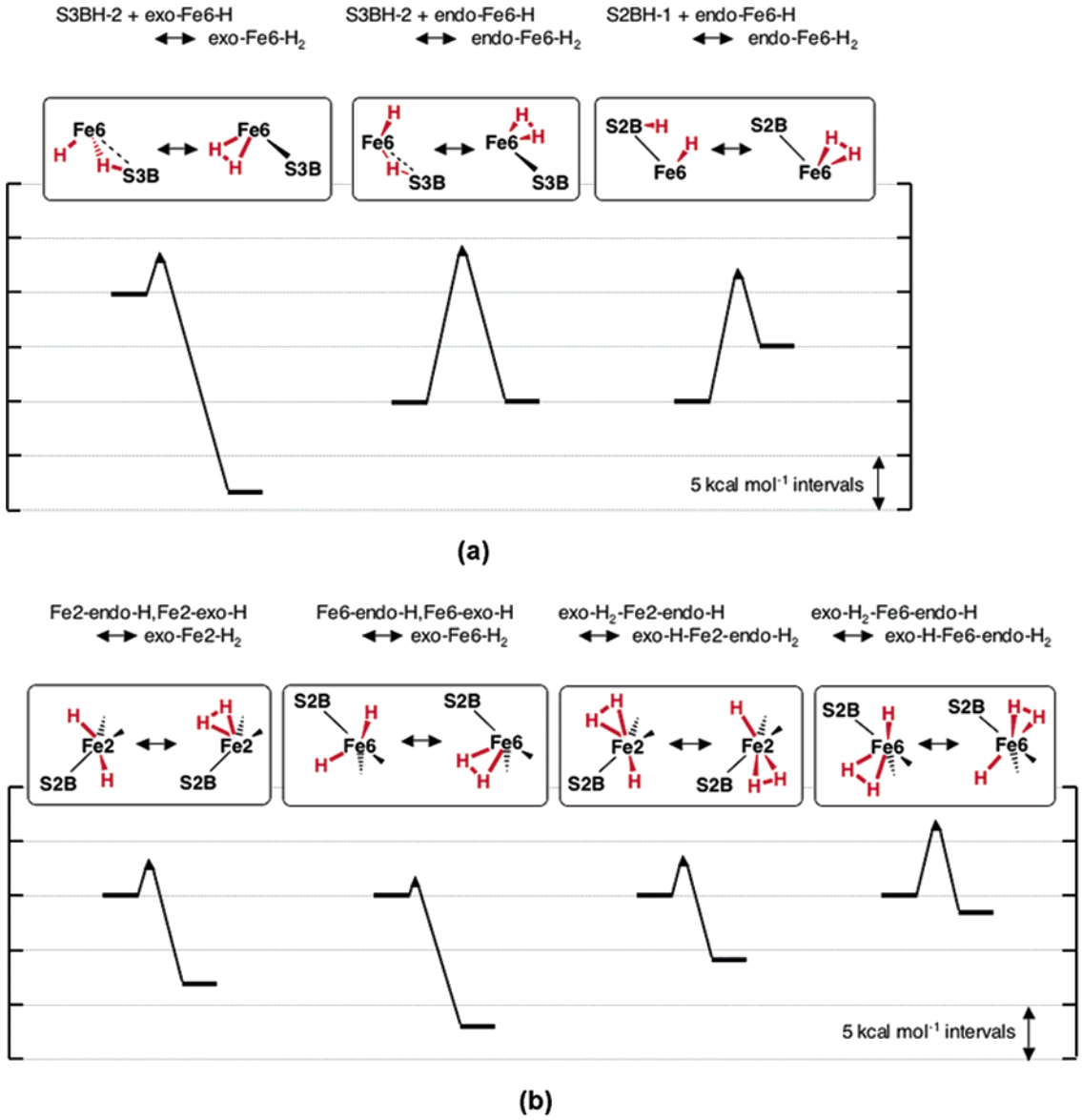

Figure 12. Energy profiles for the formation of H_2 bound to Fe. Geometrical details are provided in Figures S5, S6. (a) Transfers of H from S to Fe−H (all $S = {}^1/_2$). (b) Interconversion of $Fe(H)_2$ and Fe−H_2 (all $S = {}^1/_2$), and H/H_2 exchange on Fe (all $S = 0$). For the first H/H_2 exchange profile at Fe2, exo-Fe−H_2 has short Fe2−N^c, while for the second profile, exo-Fe6−H_2 has long (3.0 Å) Fe6−N^c.

some variation from the idealized alignments of H_2 (Figure 10) occurs, particularly when Fe−N^c is long. Barriers for interconversion of the twist isomers are calculated to be not more than about 2 kcal mol^{-1}, which agrees with experimental and theoretical data on organometallic dihydrogen complexes.[25] (5) The endo-parallel conformer (Figure 11) is generally unstable to either twisting of H_2 to the transverse conformer or to dissociation of H_2, but when there are additional ligands bound to FeMo-co it can be stabilized.[58] In the remainder of this paper, the name endo-Fe−H_2 refers to the transverse conformer. (6) Endo-transverse-Fe−H_2 coordination at Fe2 is characterized by unusually short (2.0 Å) Fe2−N^c and concomitant inward location of H_2 near the center of the Fe_4S_4 face, and is stable to dissociation of H_2 only in the $S = {}^3/_2$ state, in contrast to the behavior at Fe6.

Reaction profiles for association/dissociation of H_2 at Fe6 for exo and endo isomers have been calculated and are presented in section 9 together with the association/dissociation profiles for structures with bound H_2 and bound H.

The isomers exo-back-Fe−H_2 and endo-transverse-Fe−H_2 could be expected to be interconvertible through movement of the H_2 molecule around the exo-endo arc of coordination positions, with concomitant variation of the (μ-S)-Fe−(μ_3-S) angle. Calculations on this process indicated that the pair of H atoms remained bonded to Fe but not fully to each other, with H−H distances larger than the normal bonding distance of ca. 0.8 Å. Between endo-Fe−H_2 and exo-Fe−H_2, there is movement as bound H atoms rather than as a bound H_2 molecule. This interchange of Fe−H_2 and $Fe(H)_2$ leads to general consideration of the possibilities for generation of H_2 from H atoms on FeMo-co, and the reverse processes.

(6) How Can H_2 be Generated on FeMo-co? The formation of Fe−H_2 has been characterized for four possible processes: (a) μ_3-SH + exo-Fe−H ⟹ exo-Fe−H_2; (b) μ_3-SH + endo-Fe−H ⟹ endo-Fe−H_2; (c) μ-SH + endo-Fe−H ⟹ endo-Fe−H_2; and

(58) Dance, I. G., in preparation for publication.

(d) conversion of $Fe(H)_2$ to FeH_2. Of the three transfers from SH to Fe6−H to form Fe6−H_2, profiled in Figure 12a, the transfer from **S3BH-2** to **exo-Fe6−H** is more exergonic and has lower barrier (3 kcal mol^{-1}) than the other two, and is expected to be a very favorable mechanism for the formation of bound H_2. In contrast, combination of **endo-Fe6−H** and **SB3H-2** has a barrier of 14 kcal mol^{-1}, and the H_2 formed remains bound to Fe6 only if Fe6−S3B shortens in the early stages of the process. Geometrical details of this, and the other processes shown in Figure 12, are provided in Figures S5, S6. Transfer of H from μ-SH to Fe−H to generate bound H_2 is more favorable for endo-Fe−H than for exo-Fe−H. Figure 12a shows the profile for **S2BH-1** plus **endo-Fe6−H**, which is endergonic with a barrier of 12 kcal mol^{-1}.

The H transfers from S3B to form Fe6−H_2, with or without dissociation of H_2, are clearly relevant to early stages in the nitrogenase mechanism (Scheme 1).

(7) The $Fe(H)_2$ ⇔ $Fe(H_2)$ Interconversion. Dihydride ⇔ dihydrogen interchange is well known in hydrogen coordination chemistry, and it occurs on FeMo-co between endo-FeH,exo-FeH and exo-Fe−H_2. Energy profiles at Fe2 (involving short exo-Fe2−H_2) and at Fe6 (involving long exo-Fe6−H_2) are presented in Figure 12b, with geometrical information in Figure S6. Starting from the separated H atoms of endo-FeH,exo-FeH, the transition state occurs in a relatively flat region of the potential energy surface, with H atoms separated by 1.3−1.7 Å, and thereafter the two H atoms move as such around the endo-exo arc without formation of the final H−H bond until the exo coordination position is reached. That is, the driving force for movement to the exo position is greater than that for H−H bonding. Part of the reason for this will be the energy gain due to relief of the foldback strain of S2B when one of the H atoms is endo. In the examples shown in Figure 12b, the dynamics of the interchange favor the Fe−H_2 extreme.

Many conventional metal complexes and organometallic molecules containing hydrogen demonstrate stable structures somewhere between the M−H_2 and $M(H)_2$ extremes, with experimental H--H distances ranging from 0.8 to 1.6 Å.[24−26] The results presented here indicate that the central Fe atoms of FeMo-co can support both the Fe−H_2 and the $Fe(H)_2$ extremes as distinct structures, rather than one stable intermediate structure. Further, 'oxidative' addition of H_2 at a central Fe is unlikely for FeMo-co because exo-Fe−H_2 is more stable than $Fe(H)_2$, and the barrier for the reverse process, $Fe(H)_2$ ⇒ exo-Fe−H_2, is quite small.

(8) Structures with Fe−H_2 and Additional H Atoms. Structures in which H_2 is bound together with additional H atoms correspond to H_2 bound to reduced forms of FeMo-co, and are significant because it is in these reduced forms (E_3, E_4) that the nitrogenase activity occurs and H_2 is evolved. It is important to understand conditions that allow H_2 to remain bound or to be released at the E_3, E_4 levels, and these are examined in this section.

More than 30 combinations of H_2 bound to Fe with H atom(s) bound at Fe and/or S have been investigated. The key structures to be discussed here are pictured in Figure 13, while the full set of optimized structures is displayed in Figure S7, in the subgroups of (i) H_2 and H bound to the same Fe atom, (ii) H_2 and H bound to different Fe atoms, (iii) Fe2−H−Fe6 plus exo-Fe−H_2, (iv) H_2 bound to Fe and H bound to S, (v) structures with H_2 and 2H, and structures with two H_2 plus H.

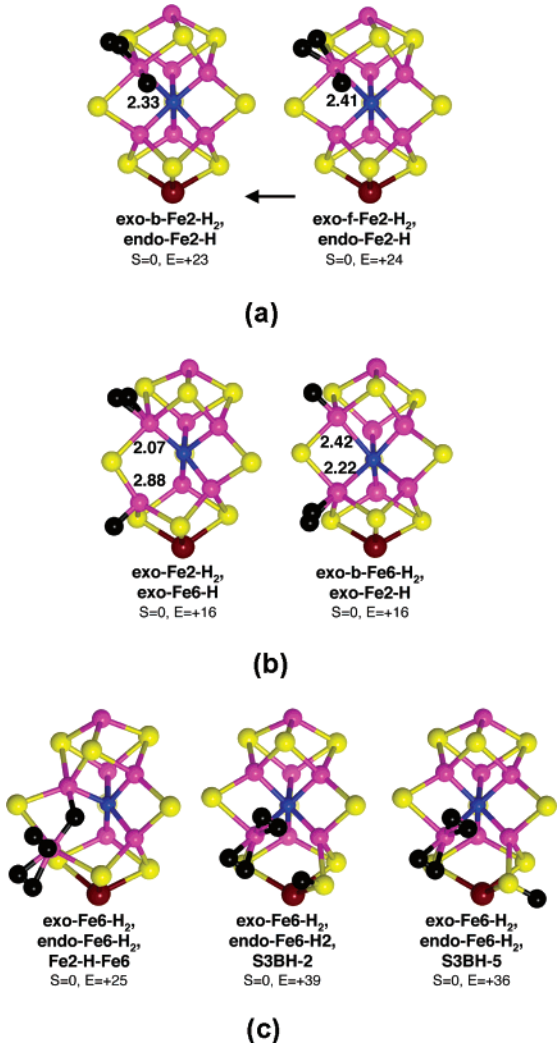

Figure 13. Selected optimized structures and isomers with H_2 bound to hydrogenated FeMo-co. The labels f and b describe the alignment of H_2 front or back, as defined in Figure 10. Relevant Fe−N^c distances are marked.

Among the structures (all $S = 0$) in which H_2 and H are bound to the same Fe atom, there are four isomers with exo-Fe−H_2 plus endo-Fe−H, and two with endo-Fe−H_2 plus exo-Fe−H. When H_2 is exo, there are isomers with short (ca. 2.35 Å) and long (ca. 3.05 Å) Fe−N^c: when H_2 is endo and H is exo, the Fe−N^c distance is intermediate, and the Fe coordination is close to octahedral. All of the optimized structures with exo-H_2 have the H_2 aligned with the back μ_3-S atom, which means that the Fe, H_2, and H atoms are approximately coplanar, which has implications for H_2/H atom exchange (see below): as shown in Figure 13a, there is barrierless conversion of the front exo-Fe2−H_2 conformer to the back conformer, with energy advantage of ca. 1 kcal mol^{-1}.

When H_2 and H are bound to different Fe atoms (Fe2, Fe6), all optimized structures ($S = 0$) have exo-H_2, and no instance of a stable structure with endo-Fe−H_2 plus exo-Fe−H on the other Fe atom has been found. Figure 13b shows the two optimized structures when both H_2 and H are in exo positions: the **exo-Fe2−H_2,exo-Fe6−H** and **exo-Fe6−H_2,exo-Fe2−H** analogous isomers have the same energy but different Fe−N^c lengths/strengths. These two structures are manifestations of

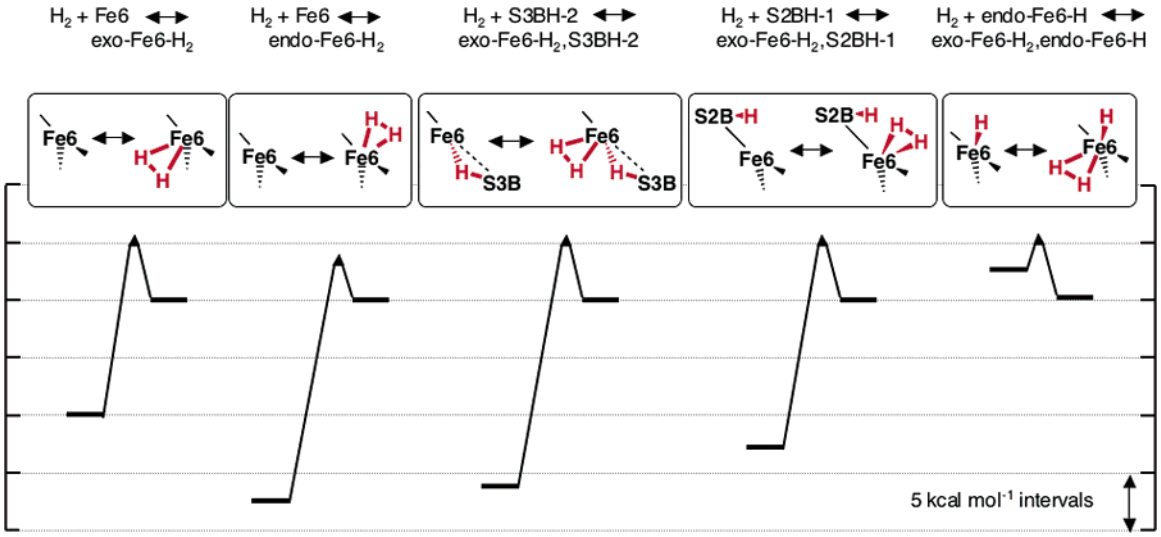

Figure 14. Energy profiles for the association/dissociation of H_2, for (left to right) **exo-Fe6−H$_2$** ($S = {}^1/_2$), **endo-Fe−H$_2$** ($S = {}^1/_2$), **exo-Fe6−H$_2$,S3BH-2** ($S = 0$), **endo-Fe6−H$_2$,S2BH** ($S = 0$), and **exo-b-Fe6−H$_2$,endo-Fe6−H** (short Fe6−N^c, $S = 0$), relative to the associated state. The dissociated states correspond, somewhat arbitrarily, to H_2 displaced by about 1 Å from the associated state.

coordinative allosterism (mutual influences of the coordinative behavior at different Fe atoms, see section 11 below) and of differences between the Fe2 and Fe6 ends of FeMo-co (see section 12 below). There are four structures (all $S = 0$) with the H atom bridging Fe2 and Fe6, and H_2 exo-coordinated on either Fe2 or Fe6, and in these the front and back conformers of H_2 both occur as local minima, in contrast to the similar structures (Figure 13a) where H is bound only to the same Fe atom that bears H_2: this is a subtle difference.

Nine structures with one H atom bonded to S and H_2 on Fe have been characterized. When the μ_3-SH bond is at the same end as Fe−H_2, only exo-Fe−H_2 coordination is possible, but this can be combined with various μ_3-SH conformations.

Further addition of H atoms and H_2 molecules to FeMo-co is possible, and indeed it is possible (in silico) to load FeMo-co with up to 12 H atoms (some as H_2), bound to each of four Fe atoms and at each of four S atoms on an Fe_4S_4 face. Obviously these extremes are not relevant to the mechanism of nitrogenase, but they demonstrate the capacity of FeMo-co for hydrogenation/reduction. Some structures that could be relevant to the E_4 and E_5 levels of the mechanism have been characterized. Among these are three that contain two H_2 molecules bound to Fe6, illustrated in Figure 13c. One of these, **exo-Fe6−H$_2$,endo-Fe6−H$_2$,Fe2−H−Fe6**, is remarkable because it attains octahedral coordination of Fe6 with complete severance of its bond to N^c. These structures increase the scope of the hydrogen chemistry of FeMo-co and, as will be shown in a subsequent report, are considered to be relevant to the mechanism of nitrogenase because one of the two H_2 molecules on Fe can be replaced by N_2.

(9) Association/Dissociation Profiles for Fe−H$_2$. The preceding structures containing H_2 are local minima on potential energy surfaces. The next questions are: which of them can readily dissociate H_2 and therefore be relevant as the intermediates that release H_2, and which of these structures can be formed by association of H_2 used as experimental inhibitor, or of D_2 in the HD reaction? We need to know the reaction profiles for association and dissociation of H_2, and how these profiles are affected by other atoms bound to FeMo-co. Accordingly, reaction profiles have been calculated for some representative types. The energy profiles are presented comparatively in Figure 14, with additional geometrical information in Figures S8, S9.

The dissociation barrier is remarkably constant at 5 kcal mol^{-1}, for H_2 bound exo or endo with or without an additional H atom on μ_3-S, μ-S, of Fe. Because the dissociated extremes in these profiles are arbitrary (generally taken as the H_2 moved by about 1 Å beyond the associated state), the association barriers are also somewhat arbitrary, but in all cases except one they are larger than the dissociation barriers and of order 10−15 kcal mol^{-1}. The significant result is that endo-H coordination decreases the association barrier for exo-Fe−H_2 to only 3 kcal mol^{-1}. This difference is reflected in the geometries of the transition states, which have Fe−H_2 = 2.3 Å for the distinctive **exo-Fe6−H$_2$,endo-Fe6−H** structure, but 1.95−2.05 Å in the others.

Further information on the influences of additional ligands on the association/dissociation profiles for Fe−H_2 comes from two structures each with two H_2 molecules bound to Fe, **exo-Fe6−H$_2$,endo-Fe6−H$_2$,Fe2−H−Fe6** and **exo-Fe6−H$_2$,endo-Fe6−H$_2$,S3BH-5**. These profiles are illustrated in Figures 15 and S9. The main observation is that the dynamics of association and dissociation of H_2 with Fe6 are now quite different from those of the less reduced molecules shown in Figure 14. In three of the four profiles, there are increased dissociation barriers, up to 18 kcal mol^{-1} for the endo-Fe6−H_2 of **exo-Fe6−H$_2$,-endo-Fe6−H$_2$,Fe2−H−Fe6**, and reduced association barriers, so that H_2 association is exergonic rather than endergonic as in the previous examples. Interpretation of the results in Figure 15 in terms of the coordination chemistry is obscure, because the two exo profiles are similar even though the trans ligands (H, N^c) are different, while the two endo profiles are quite different even though the trans ligand (μ_3-S) is the same.

Several conclusions about H_2 association/dissociation dynamics can be made at this stage. (1) As expected, other H and/or H_2 ligands can have substantial influence, and it is to be expected that other substrates, intermediates, or inhibitors will have similar

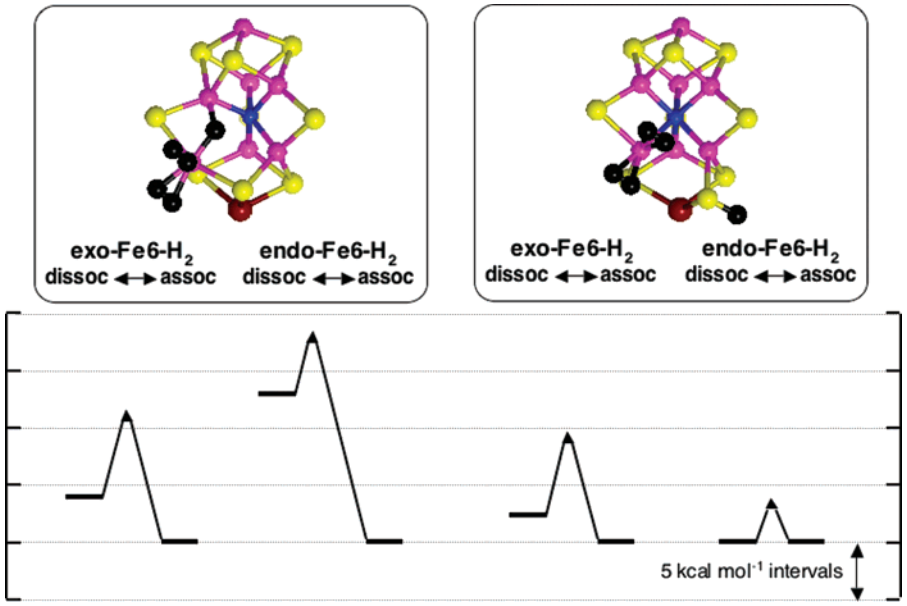

Figure 15. Energy profiles for the association/dissociation of H_2 from the exo and endo coordination positions of **exo-Fe6−H_2,endo-Fe6−H_2,Fe2−H−Fe6** and **exo-Fe6−H_2,endo-Fe6−H_2,S3BH-5** (all $S = 0$), referenced to the associated state. See Figure S9 for geometrical information.

if not larger influences on the H_2 dynamics.[59] (2) The magnitudes of barriers for association and dissociation can be in the range consistent with the various experimental data.

A few structures (**endo-Fe6−H_2,S3BH-2**, **endo-Fe6−H_2,-S3BH-5**, **endo-Fe6−H_2,exo-Fe2−H**, and **exo-Fe2−H_2,S3BH-2**) were found to be unstable to dissociation of H_2 during energy minimization, and this dissociation could not be avoided through variation of trial geometries. Generally, it is H_2 in the endo coordination position that is dissociatively unstable. The fragility of H_2 in the endo position is illustrated by **endo-Fe2−H_2,S3BH-2**, which retained H_2 in a $S = 1$ state but dissociated H_2 when $S = 0$.

(10) H/H_2 Exchange. Where H and H_2 are coordinated to the same Fe atom, there is opportunity for the H−Fe−H_2 ⇔ H_2−Fe−H scrambling reaction. Atom exchange between H and H_2 bound to the same metal atom is known in conventional coordination complexes and organometallic molecules, and is generally observed to be a facile process.[26] Two mechanisms considered in many theoretical investigations of these reactions[25,26] have either (a) the Fe,H,H_2 atoms in the same plane with the central H atom moving between the two outer H atoms, or (b) a transition state with a 3H atom set not coplanar with Fe. In section 8, it was pointed out that optimized FeMo-co structures with H_2 and H on the same Fe atom have the Fe, H_2, and H atoms approximately coplanar, and so the coplanar exchange mechanism (a) is likely. This exchange process, at Fe2 and at Fe6, has been profiled (Figure S10): the relative energies of the exo-H_2,endo-H state, the transition state, and the exo-H,endo-H_2 state are 0, +3, −6 kcal mol^{-1} at Fe2, and 0, +7, +2 kcal mol^{-1} at Fe6. The Fe−N^c distance is a variable that affects the details of the profile, but it is clear that H/H_2 exchange at Fe is a relatively facile process.

(11) Coordinative Allosterism. The binding (or lack of binding) of H_2 at one Fe atom is influenced by H or H_2 coordination at other central Fe atoms, and by hydrogenation of S. For example, endo-Fe6−H_2 coordination (profiled in Figure 14) becomes unstable to dissociation of H_2 when there is additional exo-coordination of H at Fe2. These mutual influences of binding at two different central Fe atoms of FeMo-co occur also with other substrates and inhibitors,[18,58] and this phenomenon is named coordinative allosterism. Explanations involve the bonding capacities of the relevant Fe (and S) atoms, together with a universal mechanism involving N^c, which interacts with all of the (central) Fe atoms. N^c is over-coordinated in resting FeMo-co, and so readily weakens or severs one N^c−Fe bond when there is additional ligation of the Fe, particularly strong exo-ligation. However, when there is external ligation of two or more Fe atoms, there is competition between the weakening Fe−N^c interactions, which could cause N^c to be under-coordinated or irregularly coordinated. That is, the nature of the L_A−Fe_A bonding in the sequence L_A−Fe_A−N^c−Fe_B−L_B influences the nature of L_B−Fe_B bonding, via N^c. In this way, allosteric relationships develop between these Fe coordination sites.

(12) End Differentiation in FeMo-co. In Figure 13b, the analogous structures **exo-Fe2−H_2,exo-Fe6−H** and **exo-Fe6−H_2,exo-Fe2−H** with exo-H_2 on one Fe and exo-H on the other are seen to have different distributions of Fe−N^c distances, either long + short, or intermediate + intermediate. This is demonstrating the coordinative allosterism between Fe2 and Fe6, but it is also showing that Fe and Fe6 are inequivalent. This is an instance of a general property of FeMo-co evident in the structures described in this paper, and in structures with bound substrates and inhibitors,[18,58] a difference between the Fe1 and the Mo ends of FeMo-co. In **5**, the connectivities in the red and blue enclosed regions are identical, and in the 1M1N structure there is no significant difference in the bonding geometries of corresponding atoms in the two regions. It might then be considered that Fe2,Fe3,Fe4 and their connected atoms would behave similarly to Fe6,Fe7,Fe5. However, the difference between the two ends, Fe1 is four coordinate while Mo is six

(59) Calculations in progress show that substitution of one of the H_2 molecules in exo-Fe6−H2,endo-Fe6−H2,Fe2−H−Fe6 and exo-Fe6−H2,endo-Fe6−H2,S3BH-5 by N_2 causes substantial changes in the profiles for H_2 association/dissociation.

coordinate, is transmitted through FeMo-co and causes the two ends to have some different behavior with hydrogen and with other ligands: this effect is inherent in FeMo-co and is distinct from differences due to different protein surrounds.

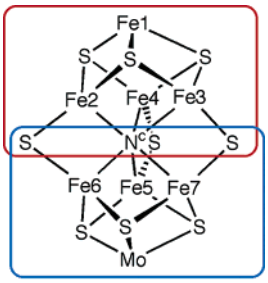

5

In the results presented in this paper, the differences between the ends are not pronounced, but occur generally. For example, the Fe2−H−Fe6 bridge is usually slightly asymmetric. In hydrogenated structures, the atoms Fe2 and S2A move further from their resting positions than do Fe6 and S3B. My interpretation of these differences is that the six-coordination of Mo is more angularly constrained than the four coordination of Fe1, restricting the stereochemical distortions of the S atoms bound to Mo, and of the Fe atoms bound to them. I suggest that this inherent differentiation of the two ends of FeMo-co could transpire to be mechanistically significant once more details of the mechanism are known, and be the reason Mo occurs in the most efficient nitrogenase enzymes.

Discussion

These DF calculations assert that H atoms and H_2 molecules can bind in numerous ways to the central Fe atoms of FeMo-co, and that H atoms can bind in varied ways to the μ_3-S and μ-S atoms, and that these binding modes can occur together. In this investigation, more than 80 structures and isomers have been characterized, together with some transformations of them. This substantially expands the scope of the hydrogen chemistry of FeMo-co, some of which is unprecedented. The most extensive previous calculations on an Fe_7MoS_9 cluster model of FeMo-co described without detail 12 models with bound H and H_2, but did not characterize any of the fundamental stereochemical changes at Fe and S, or the H-transfer processes, or the H_2 association/dissociation profiles.[39]

The results presented here provide the foundation for interpretation of spectroscopic data on hydrogenated FeMo-co in the enzyme (see below), and for development of more specific hypotheses about aspects of mechanism. This is new hydrogen chemistry. Some of the principles are common to known coordination complexes of H and H_2, which are monometallic, and there is some parallel with calculated processes for the Fe-only hydrogenase enzymes which catalyze $H_2 \leftrightarrow 2H^+ + 2e^-$ and contain two metal atoms.[60] However, the hydrogen chemistry of the multimetallic FeMo-co cluster is multivariate and unique. The key principles of the hydrogen coordination chemistry of FeMo-co, ensuing from these results, are listed in the Supporting Information.

All indications favor S3BH as the H-entry site of Scheme 3. The main conclusions concern the proton pathway to S3B, and the subsequent accumulation of hydrogen atoms and molecules on the reaction face of FeMo-co.

The Mechanism for Protonation of S3B. It is shown above that water 679 is at the terminus of hydrogen-bonded sequences that could deliver protons to FeMo-co, and that S3B is 4.0 Å from the O atom of this water molecule. In a number of the structures described above, S3B moves toward O(679). For instance, if structure **S3BH-5,Fe2−H−Fe6** (Figure 9) is superimposed on FeMo-co in 1M1N, the S3B---O(679) distance becomes 3.4 Å, which is the length of a S···H−O or S−H···O hydrogen bond. Therefore, S3B can be sufficiently mobile to accept a proton transferred via a hydrogen bond from O(679).

Figure 16a illustrates the hydrogen-bond pathway between S3B and water molecules 679, 15, 259, 24, supported by the carbonyl O atoms of α-442^{His} and α-95^{Gly}, peptide NH of α-97^{Arg}, and O5, O6, and O3 of homocitrate (see also Figure 3 for the extended water chains). The hydrogen-bond connections between O of water 679 and S3B or O5 are alternatives, and it is very unlikely for geometrical reasons that both simultaneously contain an H atom. I propose that prior to transfer of an H atom to S3B the H atoms are arranged as in Figure 16b, with the "pro-H" (blue) on water 679 docked in a hydrogen bond to O5 of homocitrate. When S3B then moves toward water 679, the H atoms move as shown by the arrows in Figure 16b, generating S3BH-5. As S3BH moves to deliver this H atom to other sections of FeMo-co (see below), a sequence of H transfers marked by arrows in Figure 16c will regenerate the pro-H on water 679, ready to repeat the transfer. Along this water chain, there are three connections (magenta arrows in Figure 16c) that can act as auxiliary proton shuttles, adjusting the acid−base details of the proton transfer. Two of these involve carboxylate/carboxyl groups of homocitrate, consistent with the strict requirements for this cofactor. The connection with O6 of homocitrate is also the route to the other water chain (Figure 3c) that could bring protons to water 259 and then to water 679 and S3B. I believe that these mechanisms are plausible for the generation of a hydrogen atom on the entry site S3B. It is significant that water 679 and water 15 have no hydrogen bonds other than those shown, that is, three each: these properties focus the H atom transfer path toward S3B.

S3BH as the H-Entry Site. Protonated S3B could exchange with solvent by reversal of the process just described. Once S3BH-5 is formed, the introduced H atom can be distributed to other sites on FeMo-co. Assuming that the Fe6/Fe2 domain is the principal locus of reactivity, the S3BH-5 structure has to pass through either S3BH-1 or S3BH-4 to S3BH-2 or S3BH-3. The barrier for this is currently estimated as 10−15 kcal mol^{-1}. When the H atom is then on the Fe6 side of S3B, it can move to endo-Fe6−H (Figure 8), and then very easily through an Fe6−H−Fe2 bridge to Fe2. Once S3B has transferred H to Fe atoms, it is able to accept another H atom from the water chain.

The possibility of different conformations for S3B−H, and variable bonding between S3B and Fe6 or Fe7, expands the functionality of the H-entry site to include H-transfer. The general unfavorability of the reverse H transfer from Fe to S3B, and in particular the large barrier for the reverse process in

(60) Peters, J. W.; Lanzilotta, W. N.; Lemon, B. J.; Seefeldt, L. C. *Science* **1998**, *282*, 1853−1858. Nicolet, Y.; Piras, C.; Legrand, P.; Hatchikian, C. E.; Fontecilla-Camps, J. C. *Structure* **1999**, *7*, 13−23. Peters, J. W. *Curr. Opin. Struct. Biol.* **1999**, *9*, 670−676. Rees, D. C. *Annu. Rev. Biochem.* **2002**, *71*, 221−246. Evans, D. J.; Pickett, C. J. *Chem. Soc. Rev.* **2003**, *32*, 268−275. Dance, I. G. *Chem. Commun.* **1999**, 1655−1656. Cao, Z.; Hall, M. B. *J. Am. Chem. Soc.* **2001**, *123*, 3734−3742. Dance, I., unpublished results.

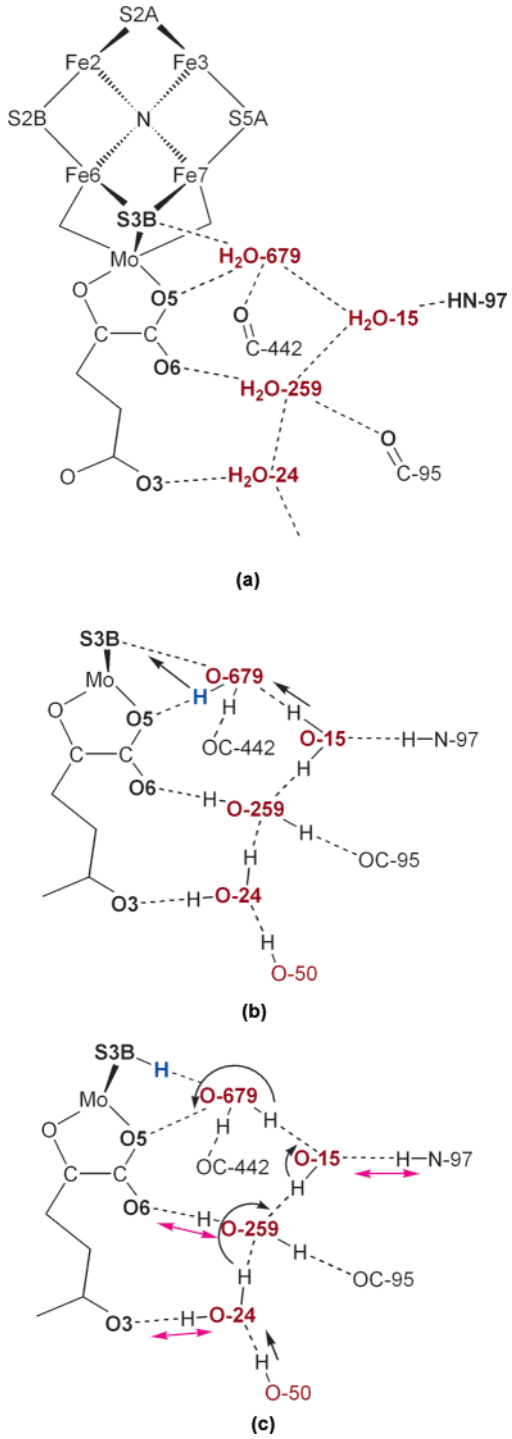

Figure 16. (a) Key components of the proposed pathway for carriage of an H atom to S3B. Only the relevant parts of homocitrate chelated to Mo are shown. The carbonyl O atoms of 442^{His} and 95^{Gly} and amide NH of 97^{Arg} are marked. The hydrogen-bond connections between O of water 679 and S3B, O5 are alternatives. Relevant angles (deg) are O15−O679−OC442, 77; O15−O679−O5, 110; OC442−O679−O5, 102; S3B−O−679−O15, 137; S3B−O679−OC442, 135; O679−O15−O259, 94; O6−O259−OC95, 103; O15−O259−O24, 144; O15−O259−O6, 97; O15−O259−OC95, 95; O24−O259−O6, 108; O24−O259−OC95, 105. (b) The proposed arrangement of H atoms prior to transfer to S3B, with the pro-H atom (blue) docked to O5, and the movements for the transfer arrowed. (c) H atom movements to regenerate the pretransfer state. The magenta arrows show H atom shuttles that could be used.

Figure 8, is consistent with the requirement of the HD reaction that isotopes in H_2 (bound to Fe) cannot reach the H-entry site. It is unlikely that an H atom on Fe6 (or Fe2) could function as the H-entry site, because this atom undergoes facile exchange with H_2 on Fe, which is contrary to the absence of exchange in the HD reaction (Schemes 2, 3). Further, the absence of water or proton donors near Fe2 and Fe6 provides no evident mechanism for the proton transfer or exchange with solvent.

Coordination Positions. The coordination positions A and B of Scheme 3 could be various combinations of exo or endo coordination positions at Fe2 and/or Fe6. Note that it is feasible that the two coordination positions could be on the one Fe atom. More than two coordination positions are possible.

The existence and properties of the structures with two H_2 bound to one Fe (Figures 13c, 15) suggest the possibility that N_2 could take the place of one of the H_2 molecules, thereby providing specific structural proposals for the associative exchange reactions of N_2 and H_2, which are key features of Schemes 1−3. These N_2/H_2 relationships occur at the E_3 and E_4 stages: if one H_2 is replaced by N_2 in these structures, they could be candidates for $E_3H_3N_2$, with ready scope for addition of a further H atom to the $E_4H_4N_2$ level. Calculations with N_2 bound to FeMo-co at various levels of hydrogenation are in progress, and it is already evident that the H_2 association/dissociation profiles of Figure 15 are modified appreciably by the substitution of N_2.

I calculate that H/H_2 exchange at Fe is a relatively facile process. This implies that HD could be formed from D_2 (by exchange rather than reduction) in the absence of N_2, which is contrary to experiment: the HD reaction is N_2-dependent. Therefore, it is suggested that in the preparation of E_3H_3 prior to N_2 coordination (Scheme 1), H and H_2 do not accumulate on the same Fe atom: the easy transfer of H between Fe2 and Fe6 provides the means for two Fe atoms to be used in this preparation.

Christiansen et al.[9] have summarized data[15,61] on the mutually inhibitory reactions of residue-substituted proteins with C_2H_2, N_2, and CO, which leads to a mechanistic model requiring at least two binding sites, one of which is more reduced. This raises questions about the differentiation of binding sites and binding states, that is, whether different locations are involved or whether one location behaves differently as reduction proceeds. Because reduction involves addition of H atoms, which may occupy Fe coordination positions, these questions are essentially about various physical locations at which H, H_2, C_2H_2, N_2, and/or CO can be bound, and how they behave at those locations and influence each other. Coordinative allosteric interactions are significant factors in this.

The Role of S2B. S2B, hydrogen bonded to 195^{His}, and possibly hydrogenated at various stages in the mechanism, is considered to function as modulator of other processes, as proposed by Durrant.[30] Modification of the S2B••α-195^{His} hydrogen bond by mutation of residue α-195 affects nitrogenase reactivity,[7,12,13,62] but the relatively large barrier for H transfer from S2B, as well as the poor path for H transfer to S2B, indicate that S2B is not likely to be the H-entry site. A possible mechanism for this modulatory function of S2B is its change in position (folding back from the front face) when there is endo-coordination at Fe6 or Fe2: in this way, interactions between S2B and protein (specifically residues α-195 and α-381) are

(61) Christiansen, J.; Cash, V. L.; Seefeldt, L. C.; Dean, D. R. *J. Biol. Chem.* **2000**, *275*, 11459−11464.
(62) Kim, C. H.; Newton, W. E.; Dean, D. R. *Biochemistry* **1995**, *34*, 2798−2808. Dilworth, M. J.; Fisher, K.; Kim, C. H.; Newton, W. E. *Biochemistry* **1998**, *37*, 17495−17505.

Scheme 4

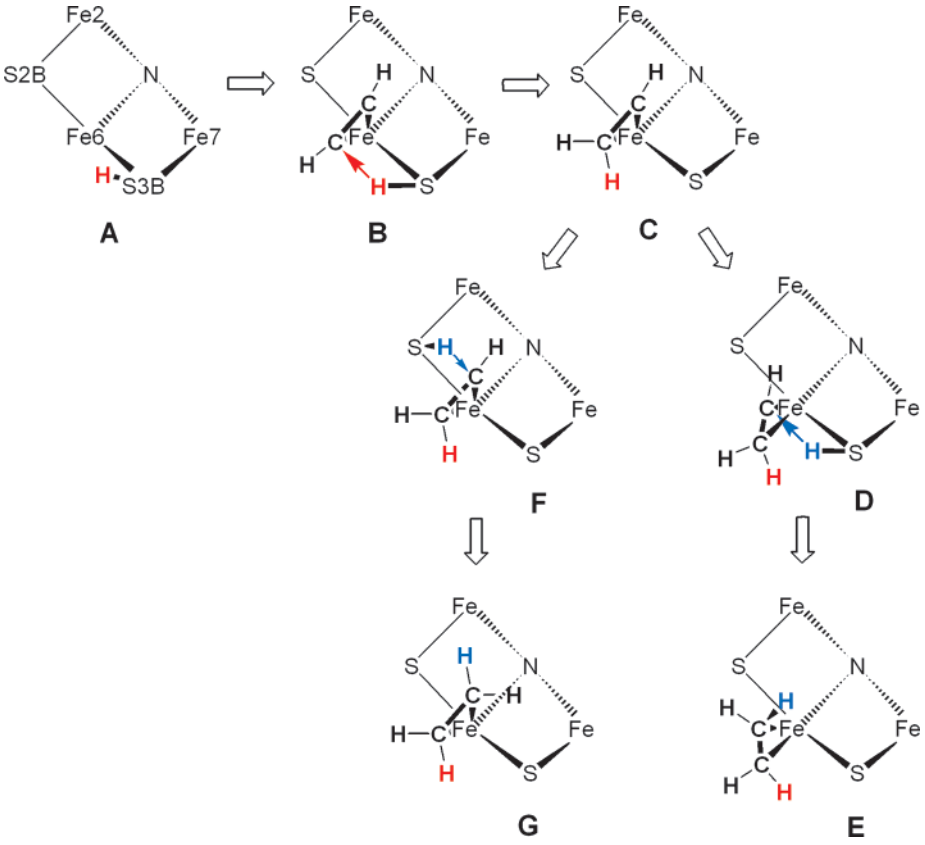

linked with coordination at Fe6 or Fe2. In the version of Scheme 2 for the E_4 level, it is suggested that S2B be hydrogenated while hydrogenated S3B functions as the H-entry site.

Substrate Hydrogenation. There is an obvious mechanism for hydrogenation of substrates bound at Fe by H transfer from S3B (and possibly S2B). Scheme 4 outlines steps by which two H atoms could be added to C_2H_2 with cis or trans stereochemistry (measured experimentally with C_2D_2[12,63]), using Fe6 as the coordination site. The **C** ⟹ **D** step involves a sliding of the bound $HCCH_2$ intermediate around the endo-exo coordination arc, so that S3BH can transfer a second H atom to the other C atom. Density functional investigations of this mechanism, and variants, are in progress.

Trapped Hydrogenated FeMo-co in the 70^{Ile} Protein. Seefeldt, Dean, and Hoffman[19] have recently reported the first trapping and spectroscopic measurement of hydrogenated FeMo-co, using the $^{Val}70^{Ile}$ mutant of the MoFe protein, in which the side-chain volume near the putative active site is increased, impeding the reduction of substrates N_2 and C_2H_2. This mutant retains full H^+ reduction activity and reveals an intermediate with a strong $S = {}^1/_2$ EPR signal, which is most probably an E_2H_2 state (Scheme 1). ENDOR measurements of this trapped intermediate have led to tentative suggestions for its structure. Relationships between the hyperfine tensors of the two bound H atoms show that they are chemically very similar. On the basis of precedent systems different from FeMo-co, models with the two H bound to S are disfavored, as are models with two terminal Fe monohydrides $(FeH)_2$; models that seemed favorable included ones with two Fe−H−Fe bridges or an Fe-dihydride, $Fe(H)_2$. The calculations described above indicate that the only Fe−H−Fe bridges that are stable are Fe2−H−Fe6 and Fe3−H−Fe7 (ignoring Fe4−H−Fe5, which is well away from the reaction face): while Fe2−H−Fe6 is likely for trapped intermediate, an Fe3−H−Fe7 bridge interferes with the S5A••96^{Arg} hydrogen bond (Figure 3a). The present theoretical investigation predicts that the trapped intermediate with two similar H atoms could have an $(SH)_2$ structure, or a $(FeH)_2$ structure, or $Fe(H)_2$. Thus, there seems to be one possibility that is supported by the experimental and theoretical approaches, that is, exo-H plus endo-H on the same Fe, and the consensual candidates for the trapped intermediate are Fe2(exo-H)(endo-H) and Fe6(exo-H)-(endo-H).

Acknowledgment. This research is supported by the Australian Research Council, the University of New South Wales, and the Australian Centre for Advanced Computing and Communications. I thank Lance Seefeldt, Dennis Dean, and Brian Hoffman for discussions.

Supporting Information Available: (a) Results assessing the accuracy of the density functional methodology, (b) reaction profiles for H-transfer reactions, (c) structures with more than one H atom, (d) isomers for H_2 bound to Fe2 or Fe6, (e) reaction profiles for the formation of H_2, (f) reaction profiles for the $Fe(H)_2 \leftrightarrow Fe(H_2)$ interconversion, (g) structures with $Fe-H_2$ and additional H atoms, (h) association/dissociation profiles for $Fe-H_2$, (i) reaction profiles for H/H_2 exchange, and (j) a list of key principles for the coordination chemistry of hydrogenated FeMo-co. This material is available free of charge via the Internet at http://pubs.acs.org.

JA0504946

(63) Dilworth, M. J. *Biochim. Biophys. Acta* **1966**, *127*, 285−294. Benton, P. M. C.; Christiansen, J.; Dean, D. R.; Seefeldt, L. C. *J. Am. Chem. Soc.* **2001**, *123*, 1822−1827.